



# The effects of peat thickness and water table depth on CO<sub>2</sub> and N<sub>2</sub>O emissions from agricultural peatlands - a process-based modelling approach

Henri Kajasilta<sup>1</sup>, Stephanie Gerin<sup>1</sup>, Milla Niiranen<sup>2</sup>, Miika Lämpikivi<sup>2,4</sup>, Maarit Liimatainen<sup>2,4</sup>, David Kraus<sup>3</sup>, Henriikka Vekuri<sup>1</sup>, Mika Korkiakoski<sup>1</sup>, Liisa Kulmala<sup>1</sup>, Jari Liski<sup>1</sup>, and Julius Vira<sup>1</sup>

<sup>1</sup>Finnish Meteorological Institute, Climate System Research, Helsinki, Finland

<sup>2</sup>Natural Resources Institute Finland (Luke), Finland

<sup>3</sup>Karlsruhe Institute of Technology, Institute of Meteorology and Climate Research

<sup>4</sup>University of Oulu, Water, Energy and Environmental Engineering Research Unit

**Correspondence:** Henri Kajasilta (henri.kajasilta@fmi.fi)

## Abstract.

Peatlands are critical carbon (C) reservoirs, storing over a fifth of the global soil organic C stock. However, some peatlands are drained and cultivated for agricultural use, which makes them a significant source of greenhouse gas (GHG) emissions. Managing water table depth (WTD) is considered a key operation for mitigating GHG emissions in cultivated peatlands.

5 Modelling the impacts of water management would be a cost-efficient way of studying its large-scale effects, both in the present and in the future. Here, we used the process-based model LandscapeDNDC (LDNDC) to assess the relationships between WTD, peat layer thickness and the GHG exchange. We simulated a boreal agricultural peatland (NorPeat, Finland), which was cultivated with silage grass and barley during the study years 2019–2022. The site was monitored with an eddy covariance (EC) tower, and divided into six drainage blocks with distinct peat profiles, each equipped with sensors for continuous water table

10 measurements. The model performance was evaluated on a daily and seasonal level using EC measurements of carbon dioxide (CO<sub>2</sub>), nitrous oxide (N<sub>2</sub>O) and water fluxes for the study years, alongside with satellite retrievals of the leaf area index and three-year data from block-specific dark chamber flux measurements of CO<sub>2</sub> and N<sub>2</sub>O. The LDNDC model was found to be suitable for drained peatland simulations, although the performance was the highest when verified against measurements from shallow peat soils. Although the simulated N<sub>2</sub>O annual balances were in the same range as the measurements, their accuracy

15 was not as high as it was for CO<sub>2</sub>. To study the impact of WTD on GHG fluxes, we had three different scenarios in addition to the baseline runs with measured conditions; these scenarios had an average WTD of 50 cm, 30 cm and 15 cm below the soil surface. The study results showed a clear relationship between CO<sub>2</sub> emissions and WTD ( $r = 0.84$  between exposed organic matter and net ecosystem carbon balance). GHG mitigation was achieved in all scenarios with increased water table; even in the most modest scenario, the annual reduction from the baseline was 0.47 kg CO<sub>2</sub>e m<sup>-2</sup> in deep peat blocks and 0.24 kg

20 CO<sub>2</sub>e m<sup>-2</sup> in shallow peat blocks. CO<sub>2</sub> emissions were found to be more strongly affected than N<sub>2</sub>O emissions. In the highest water table scenario, which resembled conditions close to paludiculture, the net ecosystem exchange of CO<sub>2</sub> became close to neutral. The implications of raising the WTD were found to be insensitive to model parameters that control evapotranspiration



or organic matter decomposition. These findings highlight that even moderate water management practices are valuable in order to mitigate GHG emissions in cultivated peatlands.

## 25 1 Introduction

Although peatlands cover only 3% of the global land surface, they have a high carbon (C) density and are therefore considered critical C reservoirs, storing 21% of the global soil organic C stock (Leifeld and Menichetti, 2018; Mander et al., 2024). In Europe, the peatlands are mainly found in the north, with Finland accounting for almost a third of peatland resources (Montanarella et al., 2006).

30 Peatlands are cultivated for their high organic matter content and ability to retain soil moisture even in drought periods. While many drained peatlands are favorable to agricultural use, cultivated peatlands are known to be a significant source of greenhouse gas (GHG) emissions (Tiemeyer et al., 2016). Pristine peatlands are naturally waterlogged, so when the peatland is drained for agriculture, it is no longer a notable source of methane (CH<sub>4</sub>) or a sink of carbon dioxide (CO<sub>2</sub>). Instead, as more organic matter (OM) is exposed to oxygen, CO<sub>2</sub> emissions increase through the microbial decomposition of peat, also  
 35 known as heterotrophic respiration (Rh), and oxidation of CH<sub>4</sub> (Evans et al., 2021). In case of nutrient-rich peat, nitrous oxide (N<sub>2</sub>O) emissions can also increase after drainage through nitrification and denitrification processes (Martikainen et al., 1993). However, CO<sub>2</sub> remains the largest contributor to the climatic impact of GHGs in drained peatlands (Dinsmore et al., 2009; Freeman et al., 2022; Gerin et al., 2023).

Raising the water table depth (WTD) has been proposed as an effective strategy for mitigating GHG emissions from drained  
 40 peatlands (Tiemeyer et al., 2016). Lång et al. (2024) in their study in Finland estimated that increasing the WTD by 0.1 m reduced the soil respiration by approximately 0.1 kg CO<sub>2</sub>-C m<sup>-2</sup> y<sup>-1</sup> over an agricultural peatland. Similarly, Evans et al. (2021) found a strong correlation between effective WTD (i.e. the average depth of the aerated peat layer) and net ecosystem productivity (NEP), which was calculated as the sum of the net ecosystem exchange of CO<sub>2</sub> (NEE) and the C removed by harvesting. Even though a clear relationship has been demonstrated between WTD and CO<sub>2</sub> emissions, the potential to reduce  
 45 N<sub>2</sub>O emissions by raising the WTD has been more difficult to assess (Wilson et al., 2016a; Couwenberg et al., 2011). N<sub>2</sub>O emissions are driven by many different abiotic and biotic processes, and these dynamics are shown to be influenced by diverse agricultural practices and meteorological events such as tilling, fertilization, and freeze-thaw cycles (Teepe et al., 2004; Maljanen et al., 2010; Wagner-Riddle et al., 2017; Wang et al., 2021; Kandel et al., 2020; Leppelt et al., 2014). In addition, the nature of N<sub>2</sub>O emissions is intermittent, i.e. short periods of high releases can contribute substantially to annual N<sub>2</sub>O emissions  
 50 (Flessa et al., 1998; Berglund and Berglund, 2011), which adds complexity in estimating and predicting N<sub>2</sub>O emissions.

Although field observations of GHG fluxes have increased in recent decades, the frequency of chamber measurements (often conducted weekly, bi-weekly if not monthly) may lead to missed seasonal dynamics and introduce high uncertainties in annual estimates (He and Roulet, 2023; Barton et al., 2015). Continuous measurements using the eddy covariance (EC) technique can address this frequency issue, but are more challenging to implement due to their complexity and high equipment costs. On the  
 55 other hand, modelling the soil processes and ecosystem responds to environmental changes is also challenging, particularly



when employing empirical approaches that rely on observations and have a limited capacity to extrapolate beyond the observed range of conditions (Duarte et al., 2003).

Cost-efficient scaling up in space and time, as well as studying the effects of alternative management actions, requires models that take into account site-specific conditions, such as peat properties, management and climate. For this purpose, we can use process-based models, which are designed to replicate the key biochemical processes occurring in the ecosystem (Cuddington et al., 2013). These models provide a mechanistic framework for understanding how various biological, physical and chemical processes (e.g., photosynthesis, decomposition, and nutrient uptake) interact and contribute to biogeochemical dynamics which drive the exchange of GHGs. Process-based models specifically adapted for organic soils (e.g. Huang et al., 2021a; Premrov et al., 2021) have been successful at simulating GHG fluxes over agricultural peatlands. However, many general land ecosystem models remain untested for simulating agricultural peatlands, even if they include the necessary process descriptions. One such ecosystem model is LandscapeDNDC (the Landscape Denitrification-Decomposition model, later LDNDC), which has been shown to accurately simulate the GHG exchange (Haas et al., 2013; Liebermann et al., 2019; Sifounakis et al., 2024) over mineral soils. The model provides a suitable basis for peat soil simulations, but its applicability has not yet been studied in northern agricultural peatlands.

The aim of this study was to assess the relationships between water table depth, peat layer thickness and GHG exchange. In addition, we wanted to determine how these relationships affect the potential of water table management to mitigate GHG emissions in northern agricultural peatlands. To address this, we had three specific research questions:

1. Is the LDNDC able to simulate daily CO<sub>2</sub> and N<sub>2</sub>O exchange in northern agricultural peatland?
2. How does a raised WTD impact the carbon balance and N<sub>2</sub>O emissions, and does the mitigation potential depend on peat depth?
3. How sensitive is the simulated WTD effect on CO<sub>2</sub> emissions to changes in parameters that determine the organic matter decomposition and soil moisture dynamics?

To tackle these questions, we simulated an intensively measured and managed peatland site that has been monitored for GHG fluxes and hydrological and chemical soil properties since 2019. We calibrated the model to reproduce the seasonal and interannual patterns in the observed GHG exchange. The study site was divided into blocks with different peat depths, which furthermore enabled us to test the simulated relationships between peat depth and GHGs. Finally, we simulated counterfactual water table depth scenarios to evaluate the potential of water management to mitigate GHG emissions on the study site.

## 2 Materials and methods

### 2.1 Site

The study site is part of the Ruukki research station located in the North Ostrobothnia (Pohjois-Pohjanmaa) region of Finland (N64°41.039' E25°6.379') and managed by the Natural Resources Institute Finland (Luke). The NorPeat facility is a ca. 27-



ha study field that is a former minerotrophic peatland drained in 1910s and cultivated since ca. 1920. The field has been continuously drained since the original drainage and drainage systems have been renewed multiple times from open ditches to subsurface drainage with wooden pipes, tile drains and modern plastic pipes. The most recent drainage works were made in 2014, when the drainage systems for each block were updated with adjustable weir to control drainage depth. Additional information on current drainage and geology of the site can be found in Yli-Halla et al. (2022).

The field is divided into eight drainage blocks, separated by a small sandy road in the center (Fig. 1). The focus is on blocks 1–6 as the detailed soil analysis was conducted only for these blocks. Blocks 1, 2 and 4 have a thicker peat layer ranging from 32 to 76 cm (on average 56 cm) while blocks 3, 5 and 6 have a thinner peat layer ranging from 16 to 56 cm (on average 34 cm). Blocks 5up and 6up have also a thinner peat layer similar to blocks 3, 5 and 6. The detailed soil properties of blocks 1–6 can be found in Table 1.

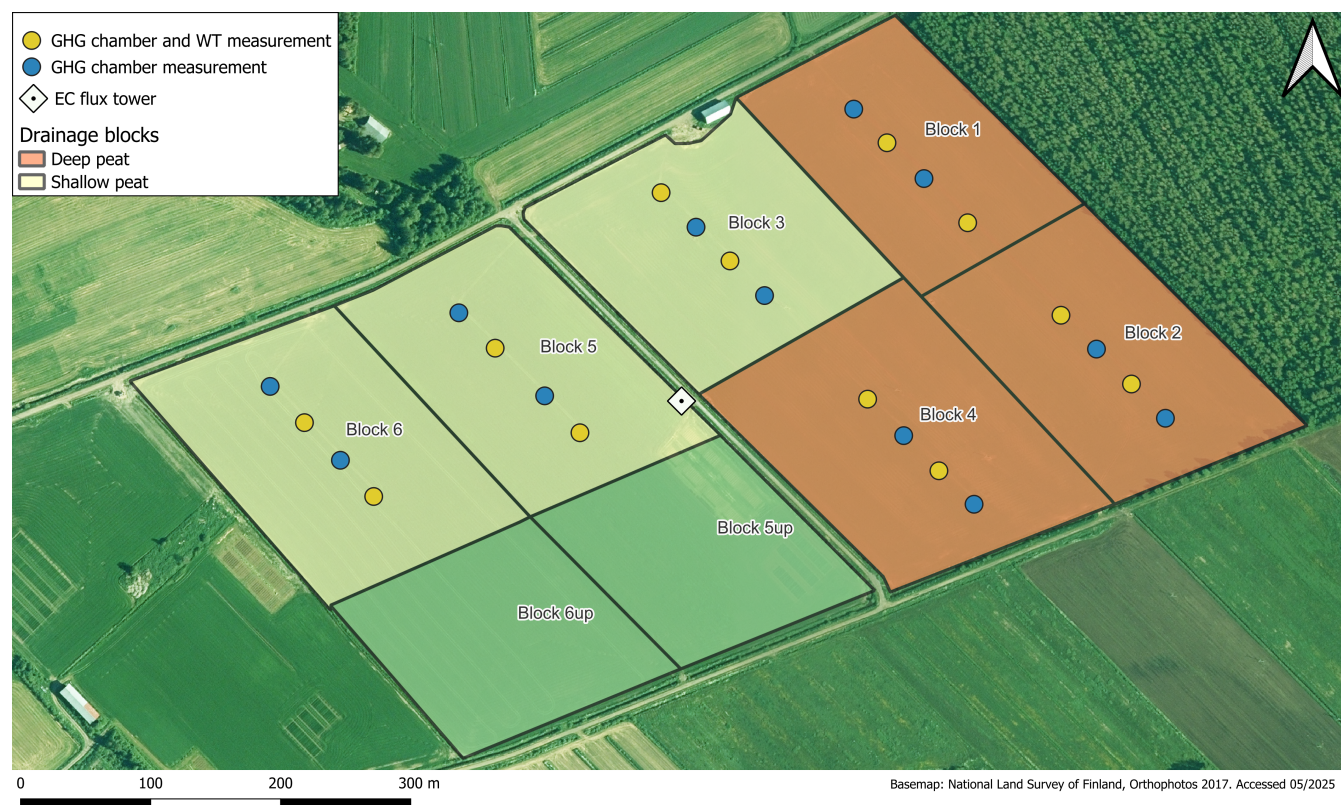


**Figure 1.** Study site with the different blocks highlighted by peat depth. Chamber measurements were done on blocks 1–6. EC measurements presented in this study include blocks 5, 6, 5up and 6up.

The site follows a traditional grass-intensive crop rotation in which grass is cultivated for three to four years, followed by one or two years of cereal crops. The sown seed mixture contained timothy (*Phleum pratense*) and meadow fescue (*Festuca pratensis*). Until fall 2021, blocks 1–4 and 5–6 were at different stages of the crop rotation. Blocks 5–6 grew perennial grasses



**Table 1.** Soil properties for each field block. C:N ratio, bulk density (BD, kg dw/dm<sup>3</sup>), carbon (C, %), nitrogen (N, g/kg) content from three sampling depths (Depth, cm) and mean peat thickness with standard deviation (Peat, cm). Original data from Yli-Halla et al. (2022) were recalculated by combining horizons. Samples were taken in 2020 from one replicate per block. WTD column shows average annual water table depth with standard deviation during 4 monitoring years used in the simulations.

Block	Depth	C:N	BD	C	N	Peat	WTD
1	0-10	19	0.475	23.7	12.6		
	10-20	18	0.475	24.2	13.1	59±9.1	77±6.3
	20-30	20	0.211	51.6	25.9		
2	0-10	16	0.49	30.7	19.5		
	10-20	16	0.49	26.8	16.7	58±11	89±17.9
	20-30	19	0.215	47.3	25		
3	0-10	17	0.522	21.9	12.7		
	10-20	17	0.205	15.3	8.8	39±7.5	93±12.1
	20-30	17	0.894	6.1	3.6		
4	0-10	17	0.62	22.8	13.8		
	10-20	17	0.62	23.5	13.9	51±7.5	78±32.2
	20-30	17	0.62	24.9	15.1		
5	0-10	17	0.611	24.6	14.5		
	10-20	15	0.214	31.1	20.3	30±7.3	84±24.9
	20-30	10	1.62	0.6	0.62		
6	0-10	19	0.657	11.9	7.8		
	10-20	20	0.647	18.1	9.1	32±5.6	106±27.5
	20-30	11	1.653	1	0.93		

from 2018 to 2021 (first sown in 2017 with triticale as a nurse crop). In blocks 1–4, barley (*Hordeum vulgare*) was first cultivated in summer 2019, then the grass mixture was grown from 2020 to 2021. Blocks 5<sub>up</sub>–6<sub>up</sub> had the same crop rotation as blocks 5–6. In September 2021, glyphosate was applied to kill the vegetation in all blocks. In June 2022, the field was first ploughed and harrowed, followed by barley sowing a few days later. In September 2022, glyphosate was applied, and in October 2022, the field was ploughed. Every year, the field was fertilized and harvested once or twice. During barley years, the field was also sprayed with herbicides (Table S8 and S9).

Based on the FMI weather station Siikajoki Ruukki, located within 1 km of our site (Finnish Meteorological Institute, 2023), the long-term 1991-2020 mean annual temperature and total precipitation were 3.2 °C and 555 mm, respectively. From 2019 to 2022, the mean annual temperatures were 3.2, 4.7, 2.4 and 3.4 °C, while the total precipitation was 519, 732, 580 and 514 mm, respectively (Fig. 2, Table S7).



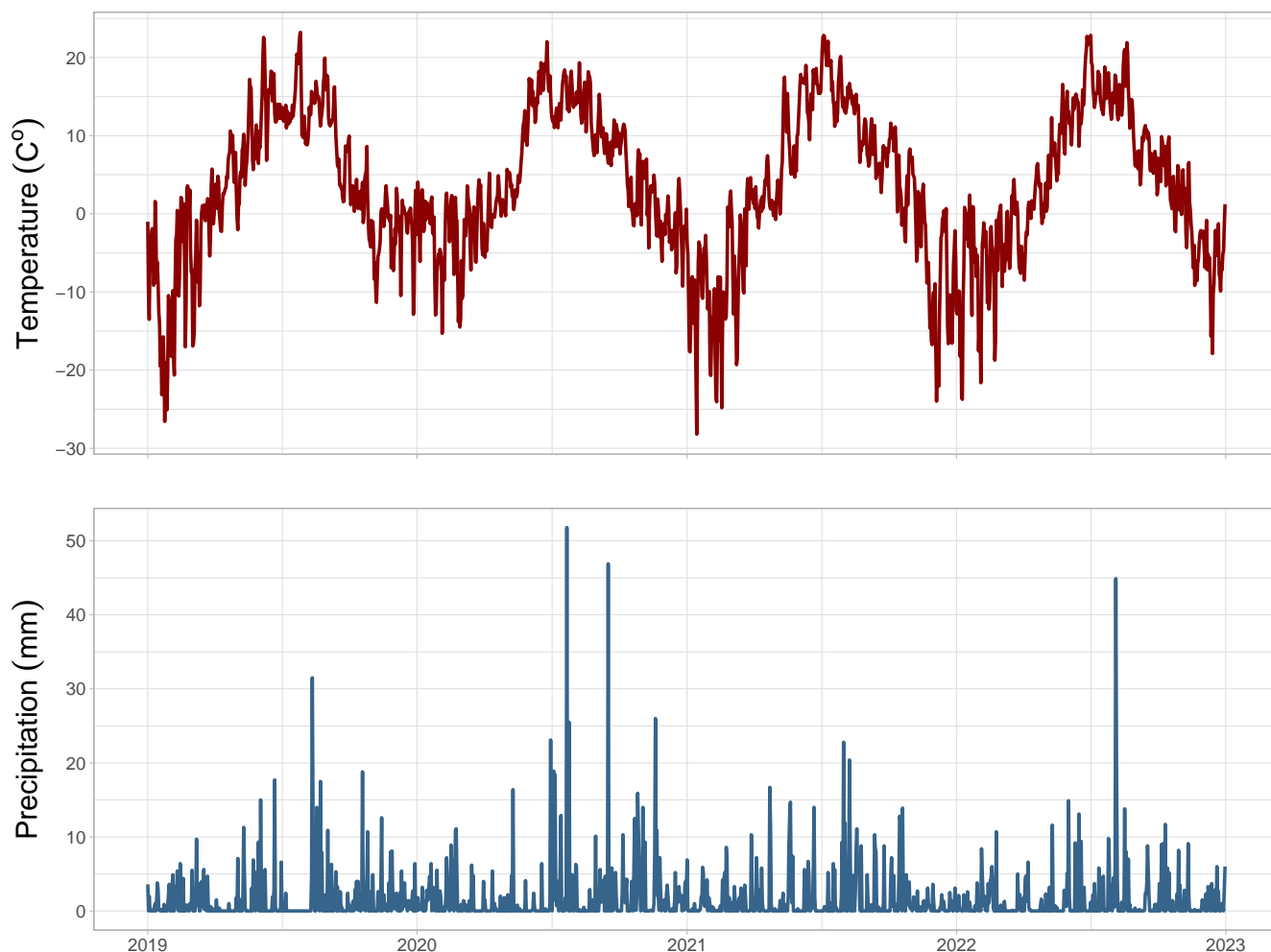


**Figure 2.** Average daily air temperature obtained from the study site and total daily precipitation obtained from the FMI weather station Siikajoki Ruukki (located within 1 km of our site) during the years 2019–2022.

## 110 2.2 Measurements

### 2.2.1 Eddy covariance measurements, filtering and gap-filling

The eddy covariance tower was installed in the middle of the field (Fig. 1) on 13 June 2019. The measurements started at a height of 2.3 m, but it was raised to 3.15 m on 25 June 2019 and to 3.3 m on 4 November 2019, where it remained until the end of the measurement period (December 2022). Since the tower installation on 13 June 2019, the EC tower was equipped  
 115 with a sonic anemometer (uSonic-3 Scientific, METEK Meteorologische Messtechnik GmbH, Germany) to measure wind speed in three dimensions and an enclosed-path non-dispersive infrared analyzer (LI-7200, LI-COR Biosciences, NE, USA)



to measure CO<sub>2</sub>/H<sub>2</sub>O mixing ratios. On 4 November 2019, a continuous-wave quantum cascade laser absorption spectrometer (LGR-CW-QCL N<sub>2</sub>O/CO-23d, Los Gatos Research Inc., CA, USA) was installed to measure N<sub>2</sub>O mixing ratio. The sampling frequency was 10 Hz, and the fluxes were averaged over a period of 30 minutes. Standard, well-established methods were used to calculate the 30-min turbulent fluxes. The details of the calculation and filtering procedures for CO<sub>2</sub> fluxes are described in Vira et al. (2025) and for N<sub>2</sub>O fluxes in Gerin et al. (2023), except for variance of N<sub>2</sub>O mixing ratio which was here set to 5.5 10<sup>-5</sup> ppm<sup>2</sup>. Due to the location of the instrument cabin and to the dominant wind direction being from the southwest, 72% of the filtered flux data came from blocks 5–6 from June 2019 to December 2022. Since there were also different crop rotations between blocks 1–4 and 5–6 (except for summer 2022), we decided not to include EC fluxes from blocks 1–4 in this study.

Gaps in CO<sub>2</sub> and H<sub>2</sub>O flux data were filled using deep ensembles of neural networks following (Vekuri et al., 2025) using air temperature, photosynthetically active radiation, soil moisture, soil temperature, vapor pressure deficit, number of days from the previous harvest and two cyclical functions describing the time of day and season (Vekuri et al., 2023) as drivers.

N<sub>2</sub>O fluxes were available from November 2019. First, gaps of two hours were gap-filled with linear interpolation. Days with at least four observations were averaged to daily integrals, while other days were discarded. Lastly, N<sub>2</sub>O daily integrals were gap-filled with a moving average (Gerin et al., 2023).

Half-hourly evapotranspiration (ET) was calculated and processed simultaneously with CO<sub>2</sub> fluxes with the Eddypro software (v. 7.0.9, LI-COR Biosciences, USA) as described in Vira et al. (2025).

### 2.2.2 Chamber flux measurements

Total ecosystem respiration (TER) and N<sub>2</sub>O fluxes were measured weekly during snow-free seasons from 2019 to 2021 using the closed static chamber method. Metal collars (60 cm x 60 cm) with water grooves were permanently installed in the soil at the depth of 20 cm near the WTD measuring points. There were four replicates in each block. During the 45-minute closure time, an opaque metal chamber with an air mixing fan was placed on top of the collar and four 20-ml gas samples were taken at 0, 15, 30, and 45 minutes and analyzed with a gas chromatograph (HP 7890 series, GC system, Agilent, USA) equipped with flame ionization (FID), electron capture detectors (ECD) and a nickel catalyst. Fluxes were calculated using linear regression.

### 2.2.3 Environmental variable measurements

Air temperature at the height of 1.6 m (Humicap HMP155, Vaisala Oyj) and soil moisture at the depth of –10 cm (ML3 ThetaProbe sensor, Delta-T Devices Ltd., Cambridge, UK) were continuously measured near the EC tower in block 5. In addition, soil moisture at –6 cm depth was measured concurrently with the chamber measurements in blocks 1–6 using an HH2 equipped with a ThetaProbe ML2x (Delta-T Devices Ltd., Cambridge, UK). WTD was monitored in blocks 1–6 using two perforated groundwater pipes installed in each block (Fig. 1) and equipped with Solinst Levellogger sensors (Solinst, Ontario, Canada), recording values at 15-minute intervals (Pham et al., under revision).

The in-situ measurements were supported by satellite retrievals of the leaf area index (LAI), which was used for evaluating the simulated vegetation dynamics. The LAI was evaluated using the methods described in (Nevalainen et al., 2022) from the level 2A reflectance data recorded by the Sentinel-2 satellites and extracted using the Google Earth Engine.



## 150 2.3 LandscapeDNDC

We employed a process-based ecosystem model known as LandscapeDNDC to conduct the simulations in this study. The LDNDC is a well-established biogeochemical model derived from the DNDC model (Gillespy et al., 2014). The LDNDC consists of several modules, each responsible for different ecosystem processes. Due to its high modularity, the model can simulate arable, grassland and forest ecosystems, the first one being the focus of this study. The model includes a layer-wise  
 155 representation of biogeochemical (carbon and nitrogen cycling) and physical (moisture and heat) processes within the soil profile. This makes it well-suited for studying how these processes respond to variations in drivers such as water table depth and how the responses are affected by soil stratification.

### 2.3.1 Model overview

In this study, we focused on the interactions between GHG fluxes, the water cycle and the growth of vegetation. We used  
 160 the Plamox module (Liebermann et al., 2019), which simulates the carbon and nitrogen cycles in vegetation as affected by soil characteristics (nitrogen uptake) and the water cycle (transpiration). The meteorological data (e.g. temperature, radiation), which Plamox uses to calculate carbon uptake, were processed for the canopy layers using the CanopyECM module (Grote et al., 2009). In addition, we used the MeTrx module (Kraus et al., 2015; Petersen et al., 2021) to simulate carbon and nitrogen cycles in the soil. In biogeochemical models such as MeTrx, soil organic matter is represented by conceptual pools with  
 165 different turnover times. These pools and their distribution cannot be measured directly, but are calibrated indirectly against observed fluxes of CO<sub>2</sub> or long-term changes in bulk soil organic matter. Typically, during a spin-up phase and under given boundary conditions (climate, groundwater, management), the pool structure is initialized such that overall soil organic matter stocks are close to equilibrium preventing artefacts from a non-ideal initial pool distribution. However, in peat soils, especially when drained, this equilibrium assumption does not hold, as soils may exhibit substantial annual losses, requiring a different  
 170 approach as described in Section 2.4.1. N<sub>2</sub>O-forming processes (nitrification and denitrification) are simulated based on substrate and oxygen availability, microbial activity and soil pH. Lastly, we used the WatercycleDNDC module (Petersen et al., 2021) to simulate soil moisture. The module handles the dynamics of water within the soil profile, i.e. the amount of precipitation intercepted by foliage, infiltration, percolation, transpiration, runoff, and possible changes in snow cover and ice content in the soil. Evapotranspiration follows the potential evapotranspiration and is limited either by the amount of surface water or  
 175 remaining potential evapotranspiration, whichever is reached first.

For this study, we applied version 1.36 of the model (revision 11770). One of the main updates in this version is the option to relax the equilibrium assumption by the possibility to prescribe an annual target value of organic matter accumulation or loss during the spin-up years. This was implemented by introducing the new parameter (*spinupdeltaC*) for the MeTrx submodel, which enables users to align long-term changes in simulated C pools with those derived from historical observations.  
 180 The default value of *spinupdeltaC* is 0, corresponding to the original equilibrium assumption, but it can now be set to reflect user-defined annual changes.





### 2.3.2 Parameters

We made adjustments to certain site and species parameters to improve the model performance in our simulated study site. Since all of the simulated blocks had the same changes, there were no differences in the parameterisation between the blocks.

185 We focused first on heterotrophic respiration, which was found to be underestimated compared to the observations. Therefore, we increased the decomposition rates (METRX\_KR\_DC\_HUM) of soil organic matter pools to match the respiration derived from the EC measurements. The model initialises most of the carbon and nitrogen in two pools that represent young and old organic matter, but there was a notable variation in allocation ratios for these pools between the blocks. We found it necessary to simultaneously adjust the rates for both pools: adjusting either of the pools individually resulted in spurious block-  
 190 wise variability in soil respiration, caused by differences in the initial partitioning of organic matter between the model pools. This reduced the sensitivity of respiration to differences in allocation, and therefore, enabled us to simulate the respiration fluxes in a more consistent and generally applicable way. Other changes to the site parameters were an increase of the maximum potential evapotranspiration. This matched the estimated evapotranspiration levels at the site and improved the seasonal change in the moisture levels near soil surface. Finally, we adjusted a site parameter controlling the fraction of surface water  
 195 removed by runoff over each time step. The value was selected based on the study (Yli-Halla et al., 2022), which suggested that 30% of the total drainage would be due to the surface runoff on the study site.

Among the crop-specific parameters, we made changes to both forage grasses, which we refer as grass from now on, and barley. We simulated the mixture of timothy and fescue together as a generic perennial grass during the grass years. For the grass, we adjusted parameters handling the photosynthesis activity (H2OREF\_A) and stomata closing (H2OREF\_GS) at  
 200 drought. With default parametrisation the gross primary production stopped at some blocks (including block 5 where EC-tower was located) in the driest periods, when the soil moisture in the top soil layers dropped close to the wilting point. This was also reflected by low simulated LAI values. The drought periods were not seen in EC measurements (gross primary production, GPP) or satellite observations (LAI), and therefore parameters H2OREF\_A and H2OREF\_GS were set close to zero ( $1e-6$ ) to avoid underestimating the GPP in simulations. Furthermore, the species-dependent albedo factor (ALB) and maximum  
 205 water use efficiency (WUECMAX) were adjusted to improve the seasonal changes and annual outputs in GPP. In addition, we modified the senescence parameters to reduce overestimation of LAI and consequently photosynthesis in the simulations. Increasing senescence due to frost stress was essential for capturing the decrease in LAI at the onset of frost. Finally, the perennial grass plant type was also used to simulate weeds during pre-sow and post-harvest periods in year 2022. However, to prevent it from dominating GPP output, we set the SLAMAX parameter value for it to 2.

210 For barley, we had similar objectives for parameter changes as for grass. We modified the growing degree day (GDD) thresholds that determine when crops enter different growth stages. These adjustments were necessary to align crop phenology with local climate conditions. We also increased the decline of specific leaf area parameter (SLADECLINE) at the end of the crop life cycle to prevent overestimation of GPP during late growing season. In addition to modifying the SLAMAX and senescence parameters, we increased the harvest index in barley to simultaneously match the reported harvest levels and the  
 215 GPP derived from the EC measurements.



All modified parameters are shown alongside the model's default values in the Supplementary Table S1.

## 2.4 Model setup

We set up model simulations for the six blocks at the site for the years 2010–2022, with the years 2010–2016 set as spin-up years. Each block had four different scenarios: the base scenario representing the observed WTD and three other scenarios with manipulated WTDs, to evaluate the effect of WTD on GHG fluxes. These scenarios are described in detail later in the subsection 2.4.4. In addition, each block and its scenarios underwent runs with some site or species parameters modified to estimate the sensitivity of the model to these parameters. All runs shared the same climate data, as detailed in subsection 2.4.3. Each block had its own soil profile and management events. The initialisation and management setups remained unmodified for each scenario in order to study the effects of changes in WTD and the model parameters.

### 2.4.1 Site initialisation

Soil initialisation covered hydrology and soil composition features. Hydrological aspects were controlled with Van Genuchten parameters  $\alpha$  and  $n$  (based on Mualem (1976)), porosity, hydraulic conductivity, and the minimum water-filled pore space in the soil layer. The Van Genuchten parameters were used to reflect a typical water retention curve for peat. This process was performed iteratively by starting from literature values (Menberu et al., 2021) and evaluating the response in the simulated soil moisture. The Van Genuchten  $\alpha$  parameter ranged from 0.75 to 6.0: the lower values associated with the organic matter layers in order to reproduce the slow drainage and high water retention. The Van Genuchten  $n$  parameter, which affects the steepness of soil moisture curves, was set between 1.2–1.5 depending on soil layer and block. Even though some of the selected Van Genuchten parameters differed significantly from the values reported by Menberu et al. (2021) for peatlands drained for agriculture, the meta-analysis (Liu and Lennartz, 2019) examining the hydrology in peat soils emphasised the parameters' complex relation and stressed that bulk density and stage of decomposition can significantly affect parameter values. The meta-analysis also indicated a large variation in these parameters across the published studies. The porosity was set lower in the silt soil layers beneath the peat layers due to the fine-textured characteristic of silty soils. In the soil samples taken below the peat layers, the porosity was measured to be around 0.4, which we used as a point of reference for our estimates. Finally, the hydraulic conductivity was set to range from 0.00045 to 0.005 ( $\text{cm min}^{-1}$ ), where the highest values apply to the peat layers as the pore size and peat structure support faster water flow than in silty subsoil.

Soil carbon and nitrogen contents for each model layer were initialised based on values measured in soil samples (down to 200 cm) conducted in spring 2020 by Yli-Halla et al. (2022) (see supplement). The values for pH (4.4–6.1) and bulk density (0.15–1.65) were also from the same dataset. The annual C change during the spin-up years ( $\text{spinup}_{\text{deltac}}$ ) was set to  $-4500 \text{ kg ha}^{-1} \text{ C}$  for all blocks, which was approximately the C loss estimated on the shallow peat blocks 5 and 6 from the observed NEE and harvest yield (Gerin et al., 2023) in years 2020–2021. However, the loss of C was also affected by the parametrisation changes, and therefore resulted in larger annual C depletion, especially in the deep peat blocks where the annual loss was up to  $10\,000 \text{ kg ha}^{-1}$  in individual study years. We extrapolated the C and N amounts independently for each block to account for carbon depletion during the spin-up years; thereby aligning the simulated C and N stocks with the measurements for the



year 2020. The extrapolation was performed in the baseline setup (i.e. no water table changes or sensitivity analysis), and  
250 the resulting site setup was shared among all subsequent runs. The complete site initialisation for each block can be found  
Table S5.

#### 2.4.2 Management

All management activities for 2019–2022 were straightforward to incorporate into the model runs as the dates of the events  
and possible seed and fertilizer amounts were given. Tillage depth and cut height in the field were not specified, but we kept  
255 them consistent (20 & 10 cm, respectively) across blocks. Glyphosate was applied in autumn 2021 and 2022 to terminate the  
grass stand and the weeds; this was simulated as a harvest event where 99 % of biomass was left on the field as residue. The  
application of herbicide in July 2022 was furthermore taken into account by limiting the LAI of weeds (see Section 2.3.2).  
Additionally, due to technical limitations in handling organic fertilizers, we included the organic manure applied to some fields  
in 2019 as a mineral fertilization event, considering only the nitrogen input to the field. During the spin-up years, all simulations  
260 were run with perennial grass which was mowed twice a year.

#### 2.4.3 Meteorology

For the driver (climate) data in the simulations, we used air temperature measured near the EC tower and the other meteorological  
data from the FMI weather station Siikajoki Ruukki located within 1 km of our site (Finnish Meteorological Institute,  
2023); the shortwave radiation data was extracted from the Copernicus European Regional Reanalysis (CERRA; Ridal et al.,  
265 2024). For the spin-up years (2010–2016), we furthermore used three-hourly data extracted from ERA5 reanalysis (Hersbach  
et al., 2020). The data from different sources were converted to hourly data to match the time steps of the simulations. For  
ambient GHG concentrations, we used values of 415 ppm for CO<sub>2</sub>, 2 ppm for CH<sub>4</sub> and 330 ppb for N<sub>2</sub>O. These values are  
similar to the those measured at different locations in Finland (Met, 2025). Other air chemistry-related inputs were kept as  
default in the model.

#### 270 2.4.4 Water table depth

A prescribed WTD was used in all simulations. In the baseline simulations, the WTD was specified by a measured time series.  
Since WTD measurements were available from May 2018 onwards, we used the averaged hourly values from May 2018 to  
December 2022 to represent the missing data period (i.e., January 2010 - May 2018) in the spin-up simulations. This was done  
to provide a realistic representation of WTD variations, while taking into account seasonal changes.

275 Water table scenarios were applied to the period for which we had the measured data. In the baseline scenario, no changes  
were made to the water table, while in the first scenario, a constant 15 cm WTD was used as an input. The last two scenarios  
used scaled WTDs,  $WTD_{scale}$  which preserved the seasonal and annual hydrological variation and responses to precipitation  
events. These were created by uniformly squeezing original water table observations  $WTD_{obs}$ , with the ratio of target average



water level  $WTD_{target}$ . (30 cm, and 50 cm) and long term mean WTD  $WTD_{mean}$  below the soil surface:

$$280 \quad WTD_{scale} = \frac{WTD_{target}}{WTD_{mean}} \cdot WTD_{obs}. \quad (1)$$

Examples of the measured water table and scenarios for Block 5 are shown in Figure 3.

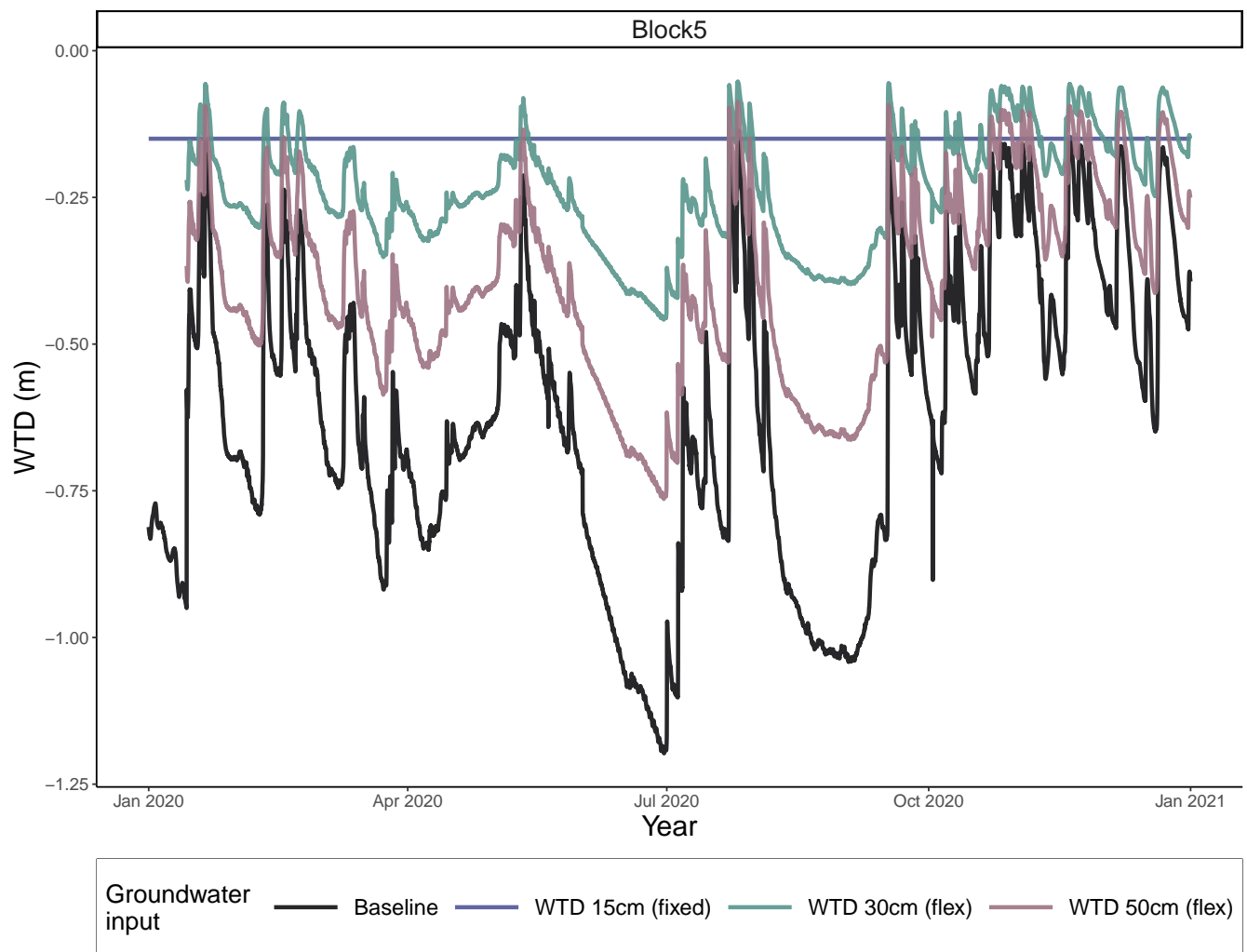


**Figure 3.** Water table depths (WTD) in year 2020 for the baseline and scenario simulations in block 5. May 2018 onward the WTDs for scenarios were on average 15 cm, 30 cm and 50 cm below soil surface. The notation *flex* (for 30 cm and 50 cm) means the scenarios followed the dynamics of the measured WTD. The notation *fixed* (for 15 cm), means that the WTD was kept consistent on given level, unless the water table was higher based on the measurement data.



## 2.5 Model evaluation and performance metrics

We evaluated the model performance for simulating NEE, N<sub>2</sub>O emission, and evapotranspiration by comparison against the EC measurements. Although the EC measurements covered the blocks 5, 5up, 6 and 6up, these measurements are addressed  
 285 only against blocks 5 and 6 as blocks 5up and 6up are not considered in this study. We furthermore compared the predicted soil water content against the field measurements and evaluated the simulated leaf area index against the satellite retrievals both described Section 2.2.3. These comparisons were performed on up to daily time resolution as determined by availability of observations.

The evaluation against EC data was supplemented by comparing the simulated ecosystem respiration against the chamber  
 290 measurements conducted across the blocks with differing peat thickness (Section 2.2.2). This comparison was based on simulated daily averages; we did not try to reproduce the 45-minute chamber closures with the model, in part because we lack mechanisms to accurately simulate short term responses of the plant respiration to temporary darkness (e.g. Tcherkez et al., 2017), and in part due to the more general uncertainties in simulating carbon allocation on a sub-daily level (Sierra et al., 2022). Although the respiration fluxes measured by the chambers are likely to differ from the daily mean, we consider this tradeoff  
 295 acceptable given that the chamber measurements are here used mainly to quantify the spatial variation of the respired CO<sub>2</sub>.

Finally, between the water table scenarios we compared the differences in heterotrophic respiration, as well as in autotrophic respiration and CO<sub>2</sub> uptake, to inspect the water table relation to these factors. We evaluated the model performance based on the metrics defined below.

### 2.5.1 Nash-Sutcliffe Efficiency

300 Nash-Sutcliffe Efficiency (NSE) is commonly used to evaluate the effectiveness of hydrological models (Krause et al., 2005). The equation for NSE is similar to the equation to calculate the coefficient of determination for regression models, where it is used to estimate the proportion of variance that the model is able to explain. The difference between R<sup>2</sup> on the regression model and NSE is the interpretation of the results. The NSE estimates the predictive power of a simulated model and focuses on the accuracy of the predictions compared to the observed values. Since the predictive values are simulated, the range of the  
 305 results varies from -infinite to 1 (perfect fit), where a value of 0 indicates that the model does not succeed any better than taking the mean value of the observations. The equation for NSE is

$$E = 1 - \frac{\sum_{i=1}^n (O_i - P_i)^2}{\sum_{i=1}^n (O_i - \bar{O})^2}, \quad (2)$$

where the  $O_i$  was observed value and  $P_i$  was simulated value. Variable  $\bar{O}$  was the mean of the observed values.





## 2.5.2 Linear regression and bootstrapping

310 We used the function `lm()` from R package `stats` (R Core Team, 2024) to quantify the linear relationship between obtained CO<sub>2</sub> values from chamber measurements and the simulated CO<sub>2</sub> values. We studied the differences in the relationships that shallow peat and deep peat had to measured values. The linear regression model was expressed as

$$O = k * S + \epsilon, \quad (3)$$

where the  $O$  was the vector of observed values and  $S$  was the vector of simulated values. Vector  $\epsilon$  included error terms as the  
 315 function seeks to minimize the sum of squared error terms by using the least square method to estimate the slope  $k$ . As seen in the equation 3, the intercept was set to 0 as we wanted to analyse the differences in the slope  $k$ . Confidence intervals (CI) for the slope difference were calculated using the R package `boot` (Angelo Canty and B. D. Ripley, 2024) with 3000 bootstrap samples.

## 2.6 Sensitivity analysis

320 An additional set of simulations was run to assess the robustness of the simulated differences between water table scenarios with respect to model parameters that influence soil biogeochemistry and water content. We perturbed three organic matter decomposition rates (METRX\_KR\_HUM 1, 2 and 3) and two parameters affecting evapotranspiration (potential evaporation fraction and WUECMAX) by individually decreasing or increasing the parameter value by 30 % of its value in the baseline simulations. These parameters are a subset of those adjusted in Section 2.3.2. Since the impact of these perturbations can be  
 325 expected to interact with the impact of the water table scenarios (Section 2.4.4), we ran the perturbed simulations separately for each water table scenario. Finally, we evaluated the response of the treatment effect (scenario versus baseline) to each parameter perturbation to provide an estimate of how sensitive the simulated GHG mitigation was with respect to the model parametrization.

## 2.7 Net ecosystem carbon balance and CO<sub>2</sub> equivalents

330 We calculated the Net ecosystem carbon balance (NECB) with the equation

$$NECB = NEE + C_{export}, \quad (4)$$

where  $C_{export}$  denotes the carbon removed in harvest. Organic fertilizers were neither simulated nor used in the years covered by the EC measurements, and thus the net carbon balance resulted only from NEE with atmosphere and harvest amounts. The  $C_{export}$  variable in the simulations were drawn from the simulated yields.

335 Finally, to study the contribution of CO<sub>2</sub> and N<sub>2</sub>O in the total climate impact of the peatland cultivation in each water table scenario, the N<sub>2</sub>O balances were converted to CO<sub>2</sub>-equivalents (CO<sub>2</sub>e) by applying the sustained global warming potential (SGWP) coefficient of 270 mol CO<sub>2</sub>e per mol N<sub>2</sub>O over a 100-yr time horizon (Neubauer, 2021).



### 3 Results

#### 3.1 Applicability of LDNDC

##### 3.1.1 Water cycle and leaf area index

To assess the model performance, we first compared the simulated water cycle and LAI in the baseline runs (driven by the measured water table depth) to the observations. The model captured the seasonal changes in the water content in the top soil layers (Figure 4; Figure S2). However, especially in block 1, a temporal shift was observed between the measurements (taken together with chamber flux measurements) and the simulations, as the measurements indicated that the soil was drier at the beginning of the summer compared to the simulation. This was also reflected in the statistics for soil moisture, as the  $R^2$  and NSE for block 1 were 0.45 and  $-0.41$ , respectively, while the same values for the rest of the blocks were 0.37–0.78 and from  $-0.03$  to 0.75, respectively. The highest  $R^2$  and NSE were obtained for blocks 5 and 6, where the EC tower flux data was also collected. Soil measurements during the winter time were unreliable and should not be emphasized due to the measurement problems when the soil is frozen or close to that point.

The evapotranspiration simulated for blocks 5 and 6 generally reproduced the seasonal variation of the EC measurements (Figure 5;  $R^2$  were 0.75 and 0.71, respectively, for these two blocks, and between 0.64–0.67 for the rest). The simulated yearly mean evapotranspiration from blocks 5 and 6 ( $1.22$ – $1.41$  mm d $^{-1}$ ) was in line with the observation ( $1.11$ – $1.20$  mm d $^{-1}$ ) for the grass years, but for the cereal year 2022 the predicted average evapotranspiration was approximately 50 % higher than the observed ( $0.96$  mm d $^{-1}$ ).

The temporal dynamics of the simulated LAI values agreed well with the observations ( $R^2$  ranging from 0.58 to 0.66; Fig. 6), as the start of the growing season and increase of LAI after the cuts were captured in the simulation. The model also captured the leaf area decline at the end of the cereal years, when the crop started to reach harvest maturity. However, even though the model predicted yearly peaks of LAI well for the grass year, the peaks at cereal years were about 40 % of the peaks retrieved from the satellite data.

##### 3.1.2 GHG fluxes and balances

The simulated TER generally agreed well with the chamber measurements ( $R^2 = 0.61$ ; Fig. 7). However, the modeled respiration fluxes were slightly underestimated for the shallow peat blocks and overestimated for the deep peat blocks. This can be seen in the regression slopes, which were above 1 ( $1.05$ – $1.13$ ; 95 % CI) for the shallow peat blocks (3, 5, 6) and slopes below 1 ( $0.84$ – $0.89$ ) for the deep peat blocks (1, 2, 4). These values differ slightly from the numbers shown in Fig. 7 as the regression lines were fitted over all of the data points from shallow and deep peat blocks. The 95 % CI for the difference between the slopes was 0.16–0.25.

The simulated daily NEE and N $_2$ O fluxes for blocks 5 and 6 followed the seasonal dynamics of the EC observations (Fig. 8). The performance with N $_2$ O fluxes were more variable than with NEE especially in late 2021 and 2022, after the glyphosate applications. The  $R^2$  values of NEE in blocks 5 and 6 were 0.58 and 0.53, respectively, and for N $_2$ O, 0.070 and 0.014,

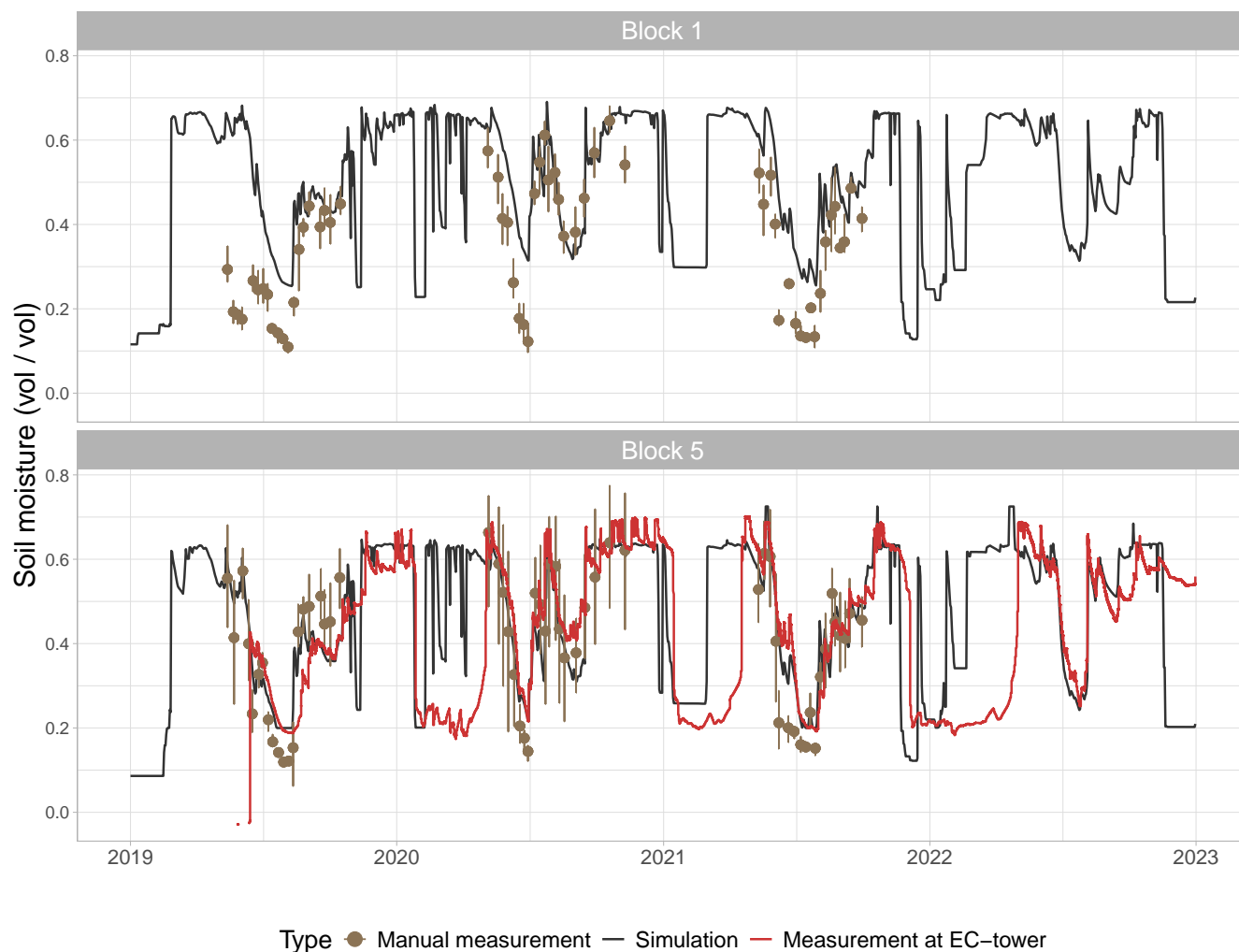


**Figure 4.** Measured and simulated volumetric soil moisture ( $\text{m}^3 \text{m}^{-3}$ ) in blocks 1 and 5. Manual measurements at the flux chamber locations are shown with round markers; simulations and measurements at the EC tower are shown with lines. Each marker for manual measurements represents the average value of four measurements taken at a given time point at a depth of 5 cm, and the error bars indicate the minimum and maximum values of these measurements. The simulations and measurements at the EC tower represent the depth of 10 cm.

370 respectively. Since the EC data did not cover blocks 1–4, comparison with continuous flux data was not possible for any deep peat blocks.

Both the model and EC observations indicated a positive annual NEE for the years 2020–2022, meaning the field was a net source of  $\text{CO}_2$ . The observed annual balances were  $0.106\text{--}0.512 \text{ kg C m}^{-2} \text{ y}^{-1}$  and the mean simulated balances were  $0.139\text{--}0.374 \text{ kg C m}^{-2} \text{ y}^{-1}$  for blocks 5–6 during 2020–2022, showing a slightly narrower range of variation compared to the  
 375 measurements. The observed (EC-tower), annual  $\text{N}_2\text{O}$  balances were  $0.48\text{--}1.31 \text{ g N m}^{-2} \text{ y}^{-1}$  while the simulated balances for

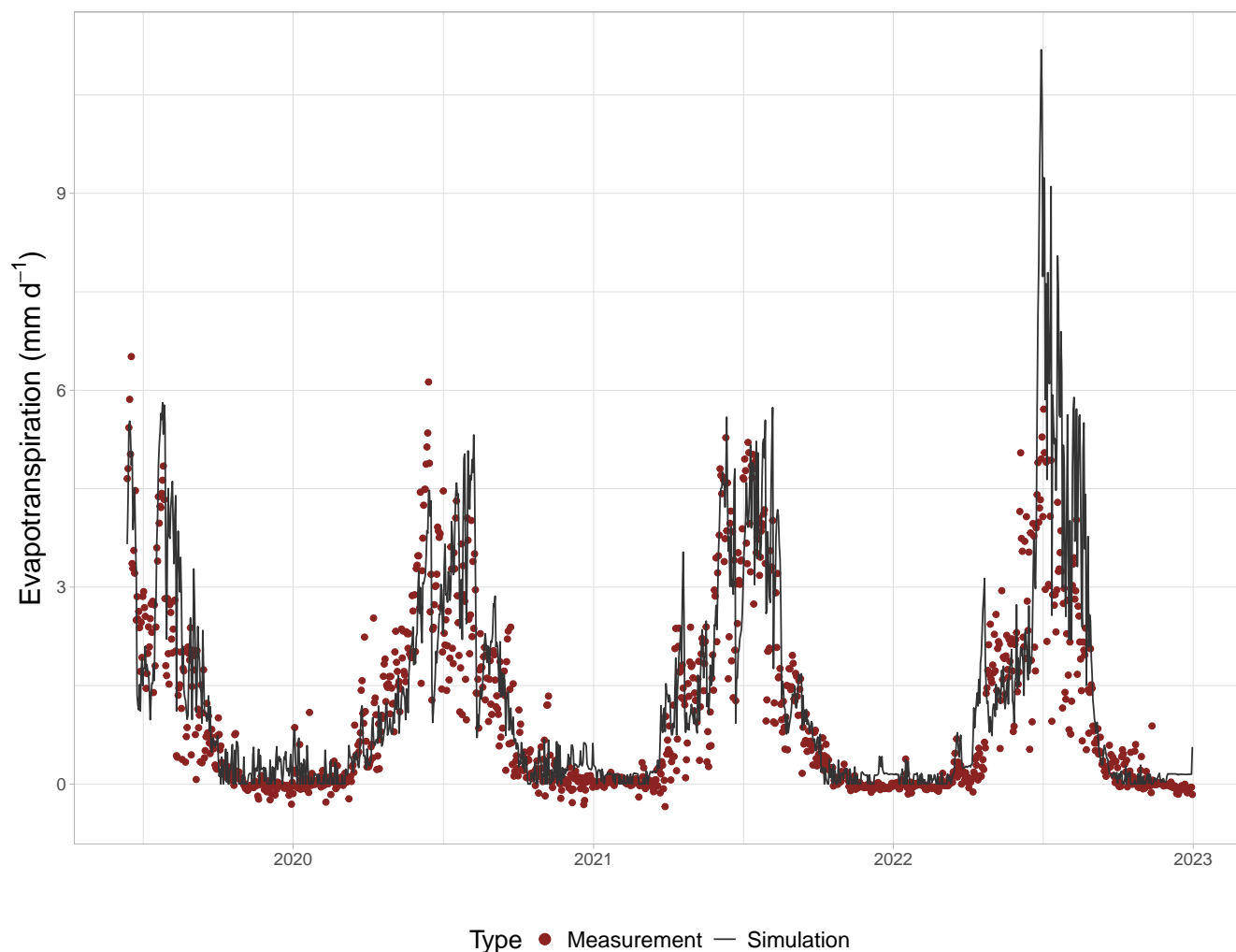


**Figure 5.** The EC measured (dots) and simulated (line) daily evapotranspiration ( $\text{mm d}^{-1}$ ) for the years 2019–2022. The simulated values are averages from blocks 5 and 6.

blocks 5 and 6 were (on average)  $0.59\text{--}1.14 \text{ g N m}^{-2} \text{ y}^{-1}$ . However, even though the ranges of balances were same magnitude, the interannual variation showed discrepancies between the measured and simulated annual balances. For the shallow peats, the highest  $\text{N}_2\text{O}$  balances were get in year 2020 (Table S3), while for measurements, the highest  $\text{N}_2\text{O}$  balance was in year 2022 (Table S4).

### 380 3.2 Water table scenarios

We compared the respiration (auto- and heterotrophic;  $R_a$  and  $R_h$ ) and  $\text{CO}_2$  uptake in baseline simulations with the scenarios involving raised WTD. The impact of water table depth raise was notable to  $R_h$ , and on average, the increase in the WTD led

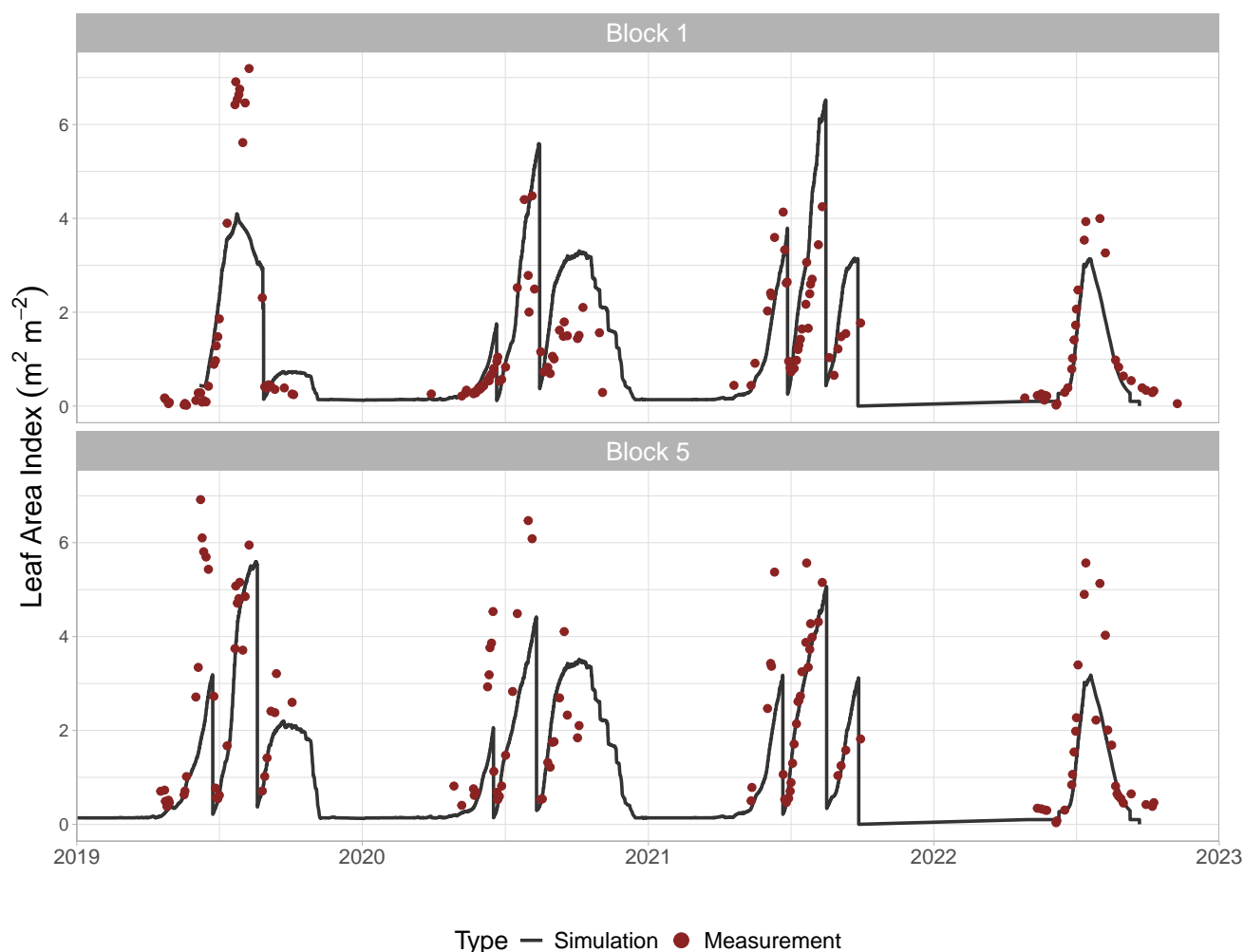


**Figure 6.** Satellite-retrieved (dots) and simulated (line) Leaf Area Index ( $\text{m}^2 \text{m}^{-2}$ ) for blocks 1 and 5 during 2019–2022.

to decrease in Rh (Fig. 9). There was more mitigation in the deeper peat blocks (1, 2, and 4) than in the shallower ones (3, 5, and 6) when the WTD was raised, as on average over the study years, for deep peat blocks, the annual Rh decreased by 0.09  
 385  $\text{kg C m}^{-2}$  (SD 0.12) in the 50 cm scenarios, 0.24  $\text{kg C m}^{-2}$  (SD 0.13) in the 30 cm scenarios and 0.47  $\text{kg C m}^{-2}$  (SD 0.1) in  
 the 15 cm scenarios. The results in shallow peat blocks were on average 0.03 (SD 0.07), 0.06 (SD 0.08) and 0.18 (SD 0.06)  
 $\text{kg C m}^{-2}$ , respectively. Standard deviations were calculated over the blocks and years. Although Rh mainly decreased with  
 increased WTD, all blocks had yearly variation with Rh sometimes increasing compared to the baseline. The changes in Ra  
 and  $\text{CO}_2$  uptake were smaller than the changes in Rh. The largest  $\text{CO}_2$  uptake changes were seen in 15 cm scenario, where  
 390 the increases were, on average, 0.09 (SD 0.07)  $\text{kg C m}^{-2}$  for deep peat blocks and 0.07 (SD 0.07)  $\text{kg C m}^{-2}$  for shallow peat



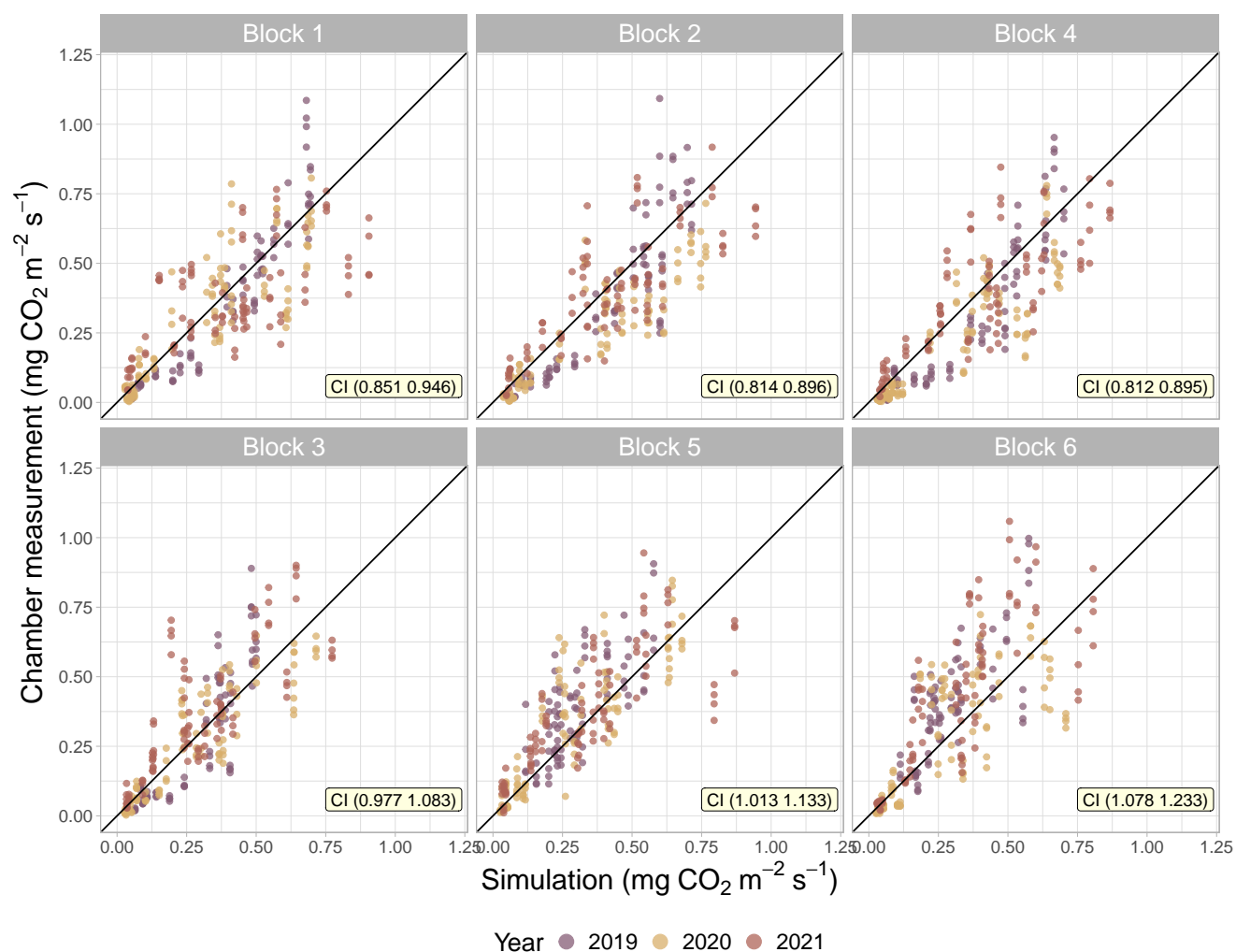


**Figure 7.** Simulated daily mean and momentarily observed total ecosystem respiration (TER) by chamber measurements in the different blocks in 2019–2021. The confidence intervals (CI) for each regression line slope are stated at the bottom right corners.



blocks. However, the net impact for carbon balance was lower as the  $R_a$  increased approximately half of the obtained increase in  $\text{CO}_2$  uptake.

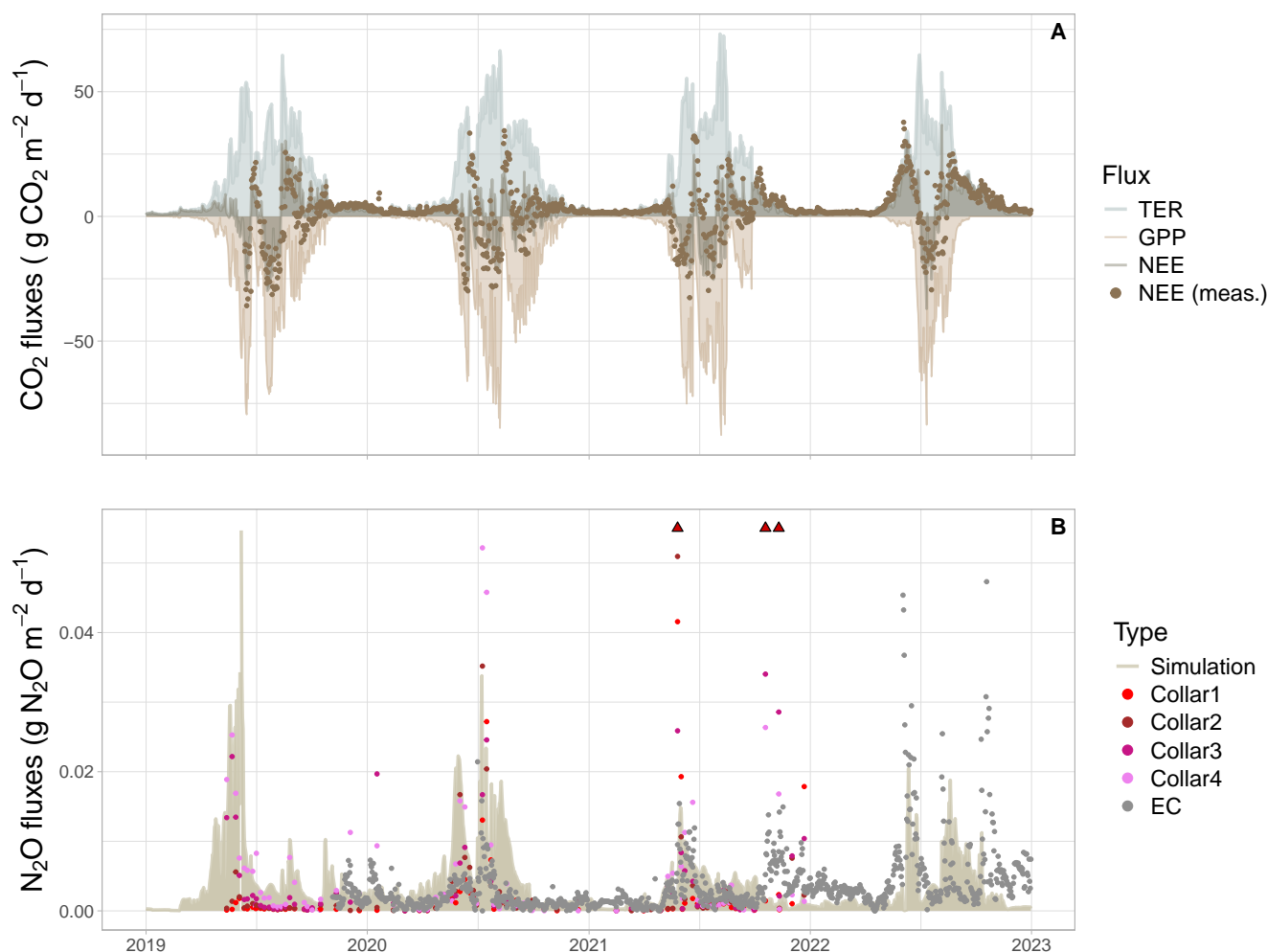


**Figure 8.** Observed (dots) and simulated (shaded areas) daily (A) net ecosystem exchange of  $\text{CO}_2$  (NEE) and (B)  $\text{N}_2\text{O}$  fluxes at the study site from 2019 to 2022. The simulated NEE is divided into gross primary production (GPP) and total ecosystem respiration (TER). Negative values indicate a sink.  $\text{CO}_2$  and  $\text{N}_2\text{O}$  fluxes were measured with the eddy covariance (EC) method, but  $\text{N}_2\text{O}$  fluxes were also measured with manual chambers, as indicated by the colored dots (B). The triangles indicate chamber measurements that were outside the scale. These outliers occurred in four instances (two of them stacked) and varied from 0.06 to  $0.21 \text{ g N}_2\text{O m}^{-2} \text{ d}^{-1}$ .



### 3.2.1 Net ecosystem carbon balance

There was a strong correlation between simulated NECB and exposed OM (i.e organic matter above WTD) ( $r = 0.84$ ), as more organic matter was decomposed in the simulations that had more OM exposed. The simulated NECB values varied due to the different scenarios, variability in species between the years, and soil profile differences among the blocks. In Figure 10 we have plotted the NECB values in relation to exposed organic matter for the baseline and all scenario simulations, as well as the estimations from measurements. The estimations were based on the NEE from EC and harvest data for years 2020–2022, and combined with the water table and soil properties (Table 1) to obtain organic matter stock above the water table. The overall variability was notable, as the annual NECB values varied from 0.10 to 1.08 kg C m<sup>-2</sup> y<sup>-1</sup>. For the three measured years, approximately 24.0 kg C m<sup>-2</sup> OM remained above the WTD. The NECB values 0.43 - 0.69 kg C m<sup>-2</sup> estimated from measurements are in line with the 18 simulated cases with a similar level (23–25 kg C m<sup>-2</sup>) of exposed OM, as the average NECB in these simulations was 0.44 kg C m<sup>-2</sup> y<sup>-1</sup> (SD 0.13).

### 3.2.2 N<sub>2</sub>O balance

Annual N<sub>2</sub>O balances in the baseline runs ranged from 0.46 to 3.14 g N m<sup>-2</sup> y<sup>-1</sup>, and on average, the deep peat blocks had larger annual emissions (1.44–2.30 g N m<sup>-2</sup> y<sup>-1</sup> on average in blocks 1, 2, 4) than the shallow peat blocks (0.68–1.13 g N m<sup>-2</sup> y<sup>-1</sup> in blocks 3, 5, 6; Table S3). The annual N<sub>2</sub>O balances were also affected by the WTD changes, and on average were reduced by 0.19 g N m<sup>-2</sup> y<sup>-1</sup> (WTD 50 cm), 0.37 g N m<sup>-2</sup> y<sup>-1</sup> (WTD 30 cm) and 0.65 g N m<sup>-2</sup> y<sup>-1</sup> (WTD 15 cm), accounting all of the blocks, in each scenario compared to the baseline.

### 3.2.3 CO<sub>2</sub> equivalents

The N<sub>2</sub>O balances were converted to CO<sub>2</sub>e and are shown together with the simulated NECB values in Figure 11. The CO<sub>2</sub>e balances were highest in the baseline runs and decreased when the WTD was raised. In the deep peat blocks, the mitigation effect was stronger (varying on average from 1.59 to 3.81 kg CO<sub>2</sub> m<sup>-2</sup> y<sup>-1</sup>) than in the shallow peat blocks (varying on average from 1.19 to 2.11 kg CO<sub>2</sub> m<sup>-2</sup> y<sup>-1</sup>). The average reduction in CO<sub>2</sub>e differed notably even when expressed relative to the change in water table depth; the largest reduction was obtained in 15 cm scenario (0.22 kg CO<sub>2</sub>-C m<sup>-2</sup> y<sup>-1</sup>) per every 0.1 m water table raise, while 30 cm and 50 cm scenarios the relative change was notably smaller (0.14 and 0.10 kg CO<sub>2</sub>-C m<sup>-2</sup> y<sup>-1</sup>, respectively). In all WTD scenarios, the share of N<sub>2</sub>O in total CO<sub>2</sub>e balances was consistent (18–20%). However, the proportion of NEE reduced (ranging from –1% to 44%) while the proportion from the harvest increased (ranging from 36% to 81%), although the harvest stayed consistent in absolute terms.

### 3.3 Sensitivity analysis

By varying the decomposition rates (METRX\_KR\_HUM) in all the original runs, the annual Rh differences ranged from –0.16 to 0.11 kg C m<sup>-2</sup> y<sup>-1</sup>. There was a large variation between the years and the blocks, but on average the largest differences were seen in the scenarios, which had the lowest water table depth i.e. most exposed organic matter. A decrease in decomposition

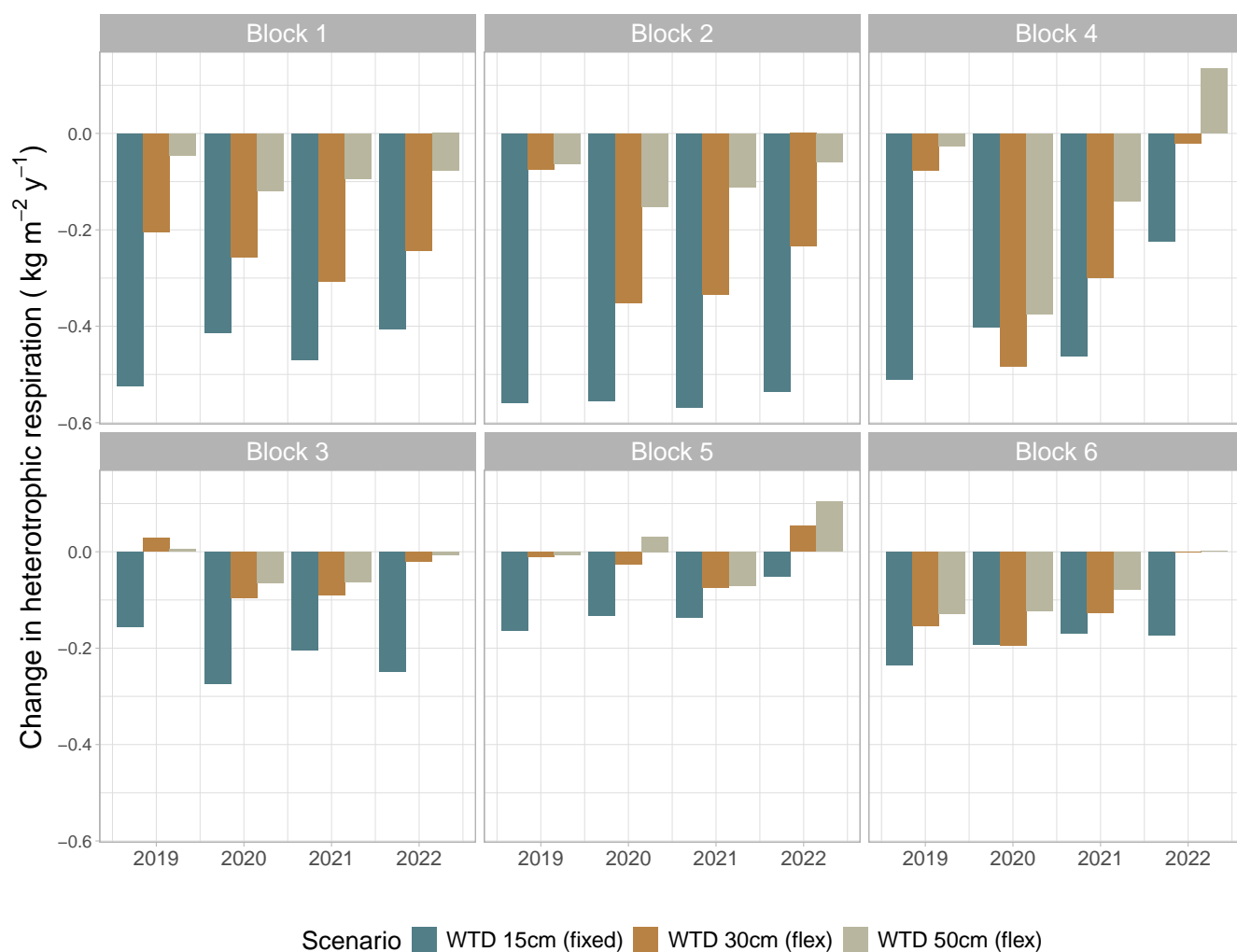


**Figure 9.** Changes in the annual heterotrophic respiration in the different blocks and at different water table depth scenarios compared to the baseline scenario. The water table scenarios are introduced in section 2.4.4 and in Figure 3.

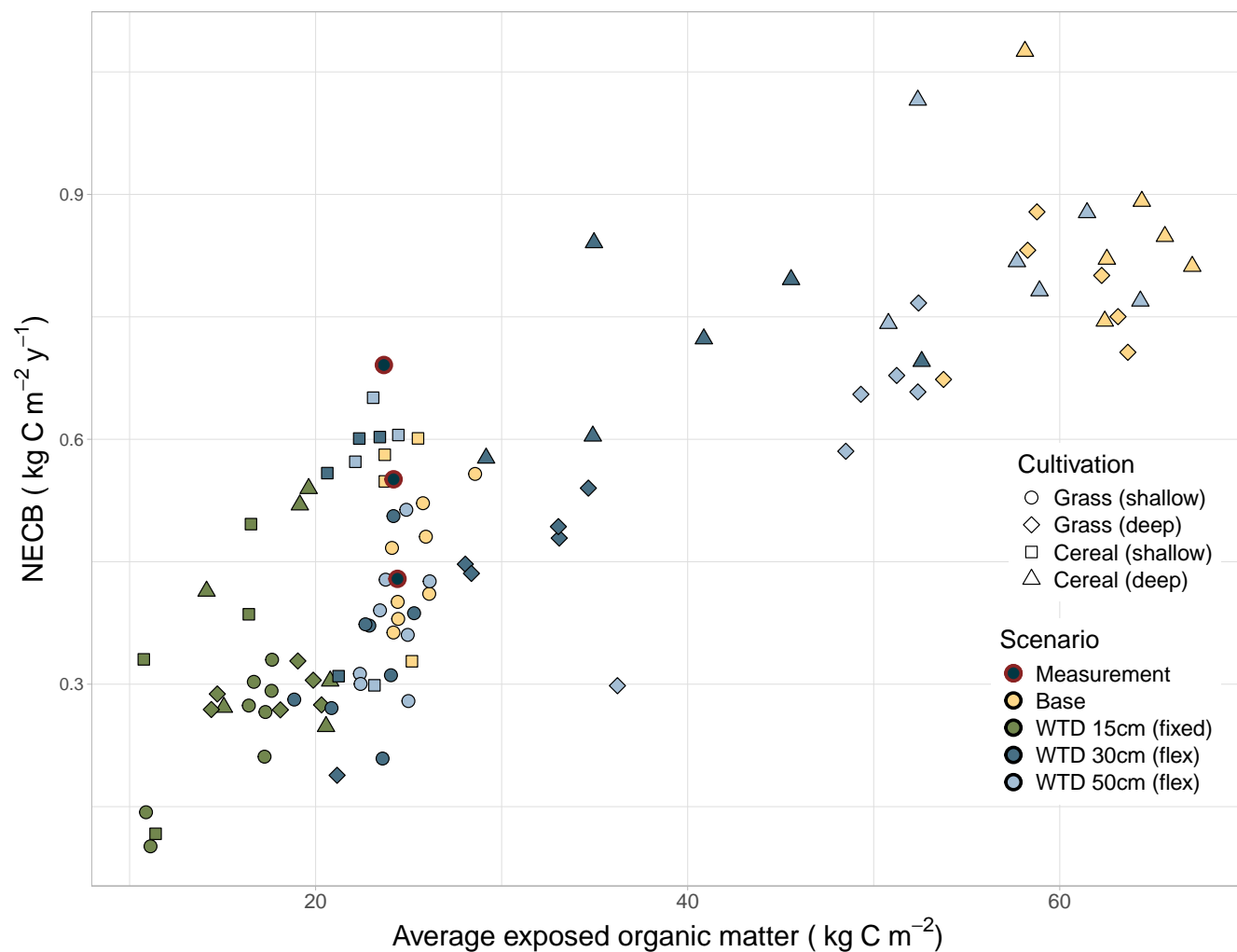


**Figure 10.** The relationship between exposed organic matter and the annual net carbon balance (NECB) in the different water table scenarios at the different blocks with different peat depths using weather drivers from 2019-2022. The estimates derived from observations are presented as black markers.





rates of the larger organic matter pools (young and old recalcitrant humus) reduced Rh by 0.04–0.12 kg C m<sup>-2</sup> y<sup>-1</sup> in deep  
 425 peat and 0.03–0.08 kg C m<sup>-2</sup> y<sup>-1</sup> in shallow peat. Conversely, increasing these rates raised Rh by 0.03–0.08 kg C m<sup>-2</sup> y<sup>-1</sup>  
 in deep peat and 0.02–0.06 kg C m<sup>-2</sup> y<sup>-1</sup> in shallow peat, depending on the scenario. For the smallest organic matter pool  
 (labile humus), the changes were minor on average, varying only from –0.02 to 0.01 kg m<sup>-2</sup> y<sup>-1</sup> as a result of increases and  
 decreases. The aggregated results of annual means and peat depth categories are shown in Figure 12. The changes in CO<sub>2</sub>  
 uptake and Ra were smaller compared to the changes in Rh, and on average over the years and blocks the CO<sub>2</sub> uptake varied  
 430 from –0.03 to 0.02 kg m<sup>-2</sup> y<sup>-1</sup>, while in Ra the variance was even smaller.

Changes in the parameter for potential evapotranspiration caused variability in Rh especially in the simulations with lower  
 WTD. For deep peat blocks, a decrease in potential evapotranspiration varied Rh from –0.05 to 0.16 kg C m<sup>-2</sup> y<sup>-1</sup>, while  
 the increase led to changes less than 0.1 C m<sup>-2</sup> y<sup>-1</sup>. In addition, the variability was only seen in the deep peat blocks, while  
 the shallow peat blocks had very minor variability. Similarly, the differences due to the changes in the water use efficiency  
 435 parameter, which was applied to perennial grasses, were generally small in Rh. On average, lowering or increasing this pa-  
 rameter would have led to only 0.01 kg C m<sup>-2</sup> y<sup>-1</sup> change in Rh. The averages for shallow and deep peat blocks aggregated  
 over the years can be seen in Figure S3. Finally, although there was annual variability, and the WTD had a leverage effect on  
 the variability, we saw in the aggregated results that on average the responses to Rh varied in parallel in the base and scenario  
 runs. Therefore, these results indicate that we would have obtained similar outcomes between the base and scenario runs, even  
 440 if the aforementioned parameter values would have been different. Overall, the emission rates would be distinct, but the effect  
 of raising the water table would still be present.

## 4 Discussion

### 4.1 Need for GHG mitigation

Drained agricultural peatlands are known to be hotspots for GHG emissions (Evans et al., 2021; Dinsmore et al., 2009; Gerin  
 445 et al., 2023), and raising the water table depth has been proposed as an effective mitigation strategy (Tiemeyer et al., 2016;  
 Freeman et al., 2022). Here, we predict that even a slight increase in the water table could reduce the negative climatic effects  
 of peatland cultivation by decreasing heterotrophic respiration and N<sub>2</sub>O emissions, particularly in areas with substantial peat  
 deposits. These results align with studies Heikkinen et al. (2024), Huang et al. (2021b) and Wilson et al. (2016b) that have  
 found the water table depth to be a key driver of CO<sub>2</sub> emissions. On the other hand, studies Leiber-Sauheitl et al. (2014) and  
 450 Eickenscheidt et al. (2015) challenge the significance of peat depth by demonstrating similar emission rates from soils with  
 different SOC stocks, consistent with studies Bridgman and Richardson (1992); Waddington et al. (2014) indicating that soil  
 respiration would be formed mainly in upper layers. Therefore, it is crucial to evaluate the performance of the model under  
 varying conditions to better understand the effectiveness and limitations of the water table management, and to ensure that  
 management decisions are based on robust, evidence-based assessments.

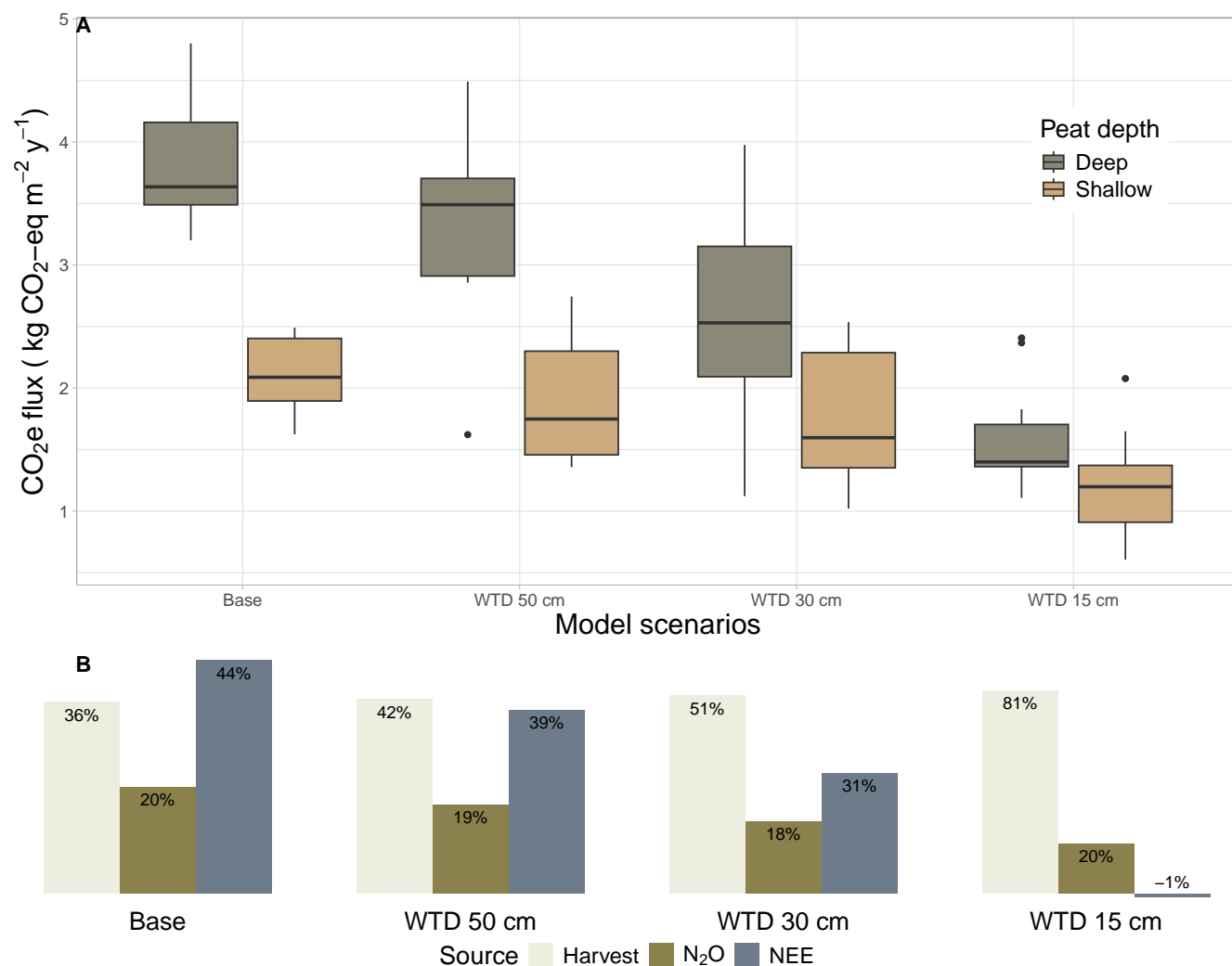


**Figure 11.** Calculated CO<sub>2</sub> equivalents (CO<sub>2</sub>e) of the baseline and the water table depth (WTD) scenario simulations with WTD raised to a specific depth (on average 15, 30 or 50 cm below the soil surface). The CO<sub>2</sub>e results are calculated from the annual NECB and N<sub>2</sub>O fluxes for years 2019–2022 for each block, with NECB as the sum of net ecosystem exchange (NEE) and the share of carbon from harvest. The results in plot (A) are shown separately for deep peat blocks and shallow peat blocks, while deep and shallow peat blocks are combined in plot (B) to show the average share of CO<sub>2</sub>e components for each scenario.

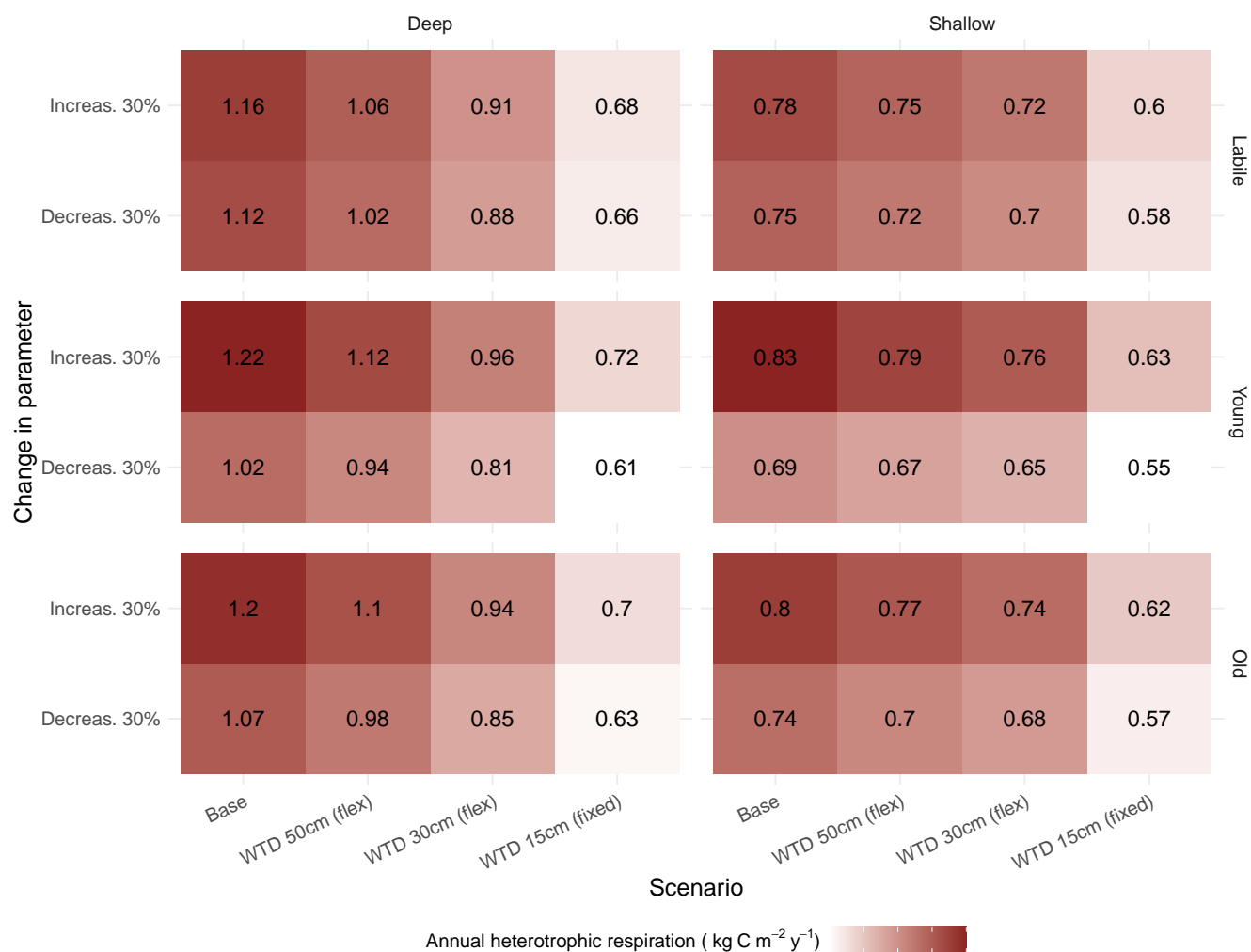


**Figure 12.** Average annual heterotrophic respiration in each water table depth (WTD) scenario for deep peat blocks and shallow peat blocks after changing decomposition rates. In the baseline run, the annual heterotrophic respiration was 1.14 kg C m<sup>-2</sup> y<sup>-1</sup> for deep peat blocks, 0.78 kg C m<sup>-2</sup> y<sup>-1</sup> for shallow peat blocks, and on average 0.96 kg C m<sup>-2</sup> y<sup>-1</sup> for all blocks.



## 4.2 Applicability of LDNDC to simulate agricultural peatlands

The model evaluation focused foremost on CO<sub>2</sub> fluxes, which are the major contributor to GHG emissions in peatlands. The simulated daily net ecosystem exchange in the shallow peat field was consistent with the EC measurements (Fig. 8a), which led to a good agreement between the simulated NECB and the estimates derived from the EC and field data (Table S3 and Fig. 10). Similar levels of agreement with observations were seen in LAI (Fig. 6) as well as soil moisture and evapotranspiration (Figs. 4 and 5). Altogether, this confirmed that the model, with the parameter modifications documented in Section 2.3.2, was suitable for simulating crop growth and CO<sub>2</sub> exchange in degraded peat soils with a shallow organic horizon.

On average, the simulated respiration fluxes were in agreement with the chamber measurements from shallow and deep peat fields. However, the simulated respiration differed between shallow and deep peat fields, which led the model to underestimate the ecosystem respiration for the shallow peat fields and overestimate it for deep peat fields.

The N<sub>2</sub>O fluxes showed more discrepancies than the CO<sub>2</sub> fluxes, and while the annual balance for one year (2021) was in line with the EC measurements, the other years were either under or overestimated by up to a factor of two. By nature, N<sub>2</sub>O fluxes are more difficult to simulate because these emissions have typically high temporal variability (Rees et al., 2013) and short-term peak emissions occur after weather and management events such as freezing-thawing or fertilization (Rees et al., 2013; Wagner-Riddle et al., 2017; Gerin et al., 2023). Even though the simulation captures many of the observed temporal patterns relatively well (Fig. 8b), the missed N<sub>2</sub>O episodes especially following the herbicide applications led to a poor quantitative agreement on a daily to seasonal level.

## 4.3 Water table depth and SOC stock as drivers of GHG emissions

Raising the water table mitigated the simulated GHG emissions in both shallow and deep fields (Fig. 11) with the greatest impact observed for CO<sub>2</sub> emissions. Peat depth and water table depth could be combined for estimating the exposed organic matter stock, which had a strong positive association with the CO<sub>2</sub> emissions (Fig. 10). A similar but weaker relationship was established empirically for cultivated peatlands in the Netherlands by Aben et al. (2024). In the simulations, the change in water table depth mainly affected the heterotrophic respiration, which was reduced even with the more conservative water table changes in this study, where the water table followed the observed seasonal variation and was only moderately higher than the measured water table (Fig. 9).

Similar to the CO<sub>2</sub> emissions, the N<sub>2</sub>O emissions were reduced when the water table was raised. Although the comparison against the EC data indicated greater uncertainties in simulating the N<sub>2</sub>O emissions compared to the CO<sub>2</sub> fluxes, this result is consistent with several empirical studies (Jeewani et al., 2025; Lång et al., 2024) and supports the hypothesis that increasing the water table can suppress nitrification and subsequently reduce the availability of nitrate for denitrification (Klemmedtsen et al., 2005; Pärn et al., 2018). The effect was still notably weaker than for CO<sub>2</sub> emissions (Fig. 11) and as the amount of carbon removed in harvest did not significantly change, the proportion of N<sub>2</sub>O emissions, relative to the total GHG burden, stayed consistent between the scenarios.



The model was parametrized primarily based on the data that represented the part of the field with a shallow peat layer, and therefore, the model results for deeper peat profiles involve additional uncertainties. Specifically, our initialization of organic matter pools did not consider differences in chemical properties of the peat layer beyond the carbon and nitrogen contents. Earlier studies, in contrast, suggest that the peat decomposition may be more strongly influenced by other aspects of peat quality, such as its polysaccharide content (Leifeld et al., 2012; Normand et al., 2021), which in turn may vary within the soil profile. The primacy of peat quality as a driver of CO<sub>2</sub> emissions is consistent with previous studies on organic soils where the CO<sub>2</sub> emissions have been found to be decoupled from the C stocks (Leiber-Sauheitl et al., 2014; Eickenscheidt et al., 2015). A difference in peat quality could also explain why the chamber measurements, contrary to the simulations, showed little or no difference in ecosystem respiration between the deep and shallow peat layers.

Altering the decomposition rates was necessary in this study to achieve comparable CO<sub>2</sub> fluxes with the observations. The sensitivity analysis with respect to these parameters indicated that even by varying the key parameters in the model, similar mitigation effects were achieved in CO<sub>2</sub> by raising the water table depth as with our initial parametrisation. In addition, we varied two parameters related to the water cycle (potential evapotranspiration and water use efficiency). Also these parameter changes had a minor impact on the mitigation potential. This sensitivity analysis showed that our findings regarding of the CO<sub>2</sub> emissions were more robust to parametrisation than the absolute CO<sub>2</sub> emissions.

#### 4.4 Potential to mitigate GHG emissions with water table management

Combining the need to harvest biomass with the need to mitigate emissions creates a strong constraint for cropland management, requiring large changes in agricultural practices and local water management. The largest reduction of GHG emissions was here achieved in the scenario with average 15 cm water table depth, which implies conditions close to those typical in paludiculture. In this case, the net exchange of CO<sub>2</sub> was close to neutral regardless of the peat layer thickness. This scenario had a permanently high water table, and did not account for seasonal variation. In practice, seasonal variation of the WTD exposes more soil organic matter to aerobic conditions during the warm season, potentially increasing the CO<sub>2</sub> emissions from soil (Heikkinen et al., 2024). This highlights the need to target water level management during summer months for maximum mitigation.

Nonetheless, the simulations also indicated that small but positive GHG mitigation is possible with less drastic changes to the water table management. The scenario with a 50 cm average WTD required on average a 31 cm higher water table for deep peat blocks and a 44 cm higher water table in shallow peat blocks. This increase in water table level can be achievable with a controlled drainage system and is unlikely to cause issues for conventional agriculture (Salla et al., 2024). In our simulations, this scenario resulted in an annual reduction of GHGs equivalent to approximately 0.47 (deep peat layers) to 0.24 (shallow peat layers) kg CO<sub>2</sub>e m<sup>-2</sup>, and in this scenario each 10 cm raise of water table levels reduced annual emission on average by 0.10 kg CO<sub>2</sub>e m<sup>-2</sup>. Such a change in long-term average WTD is sufficient for modest mitigation in emissions (Evans et al., 2021; Lång et al., 2024). Somewhat surprisingly, the emissions were reduced even in the simulations with the average WTD very close to or below the organic soil horizon in the shallow peat blocks. As the controlled drainage offers multiple benefits, such





520 as reduced nutrient leaching (Carstensen et al., 2020) and increase in available water for plants (de Wit et al., 2022), a minor climate benefit is a worthwhile addition if conversion to a more climate-neutral land use is not possible.

The water table scenarios used in the simulations were not tied to any specific water management practices, such as ditch blocking, controlled drainage or subsurface irrigation. While we evaluated the mitigation potential related to peat depth under idealized scenarios, in practice, GHG mitigation efforts are limited by local climate, hydrogeology, and drainage management practices (Boonman et al., 2022). Ideally, these aspects would be incorporated into the model structure to establish the site-specific mitigation potential.

## 5 Conclusions

Raising the water table depth was found to be an effective way of reducing emissions even in shallow peat fields. Overall, the simulation results showed a clear association between the stock of exposed organic matter and CO<sub>2</sub> emissions, indicating that even moderate changes to water management practices can help mitigate greenhouse gas emissions. We found that the LDNDC model could be adapted to simulate agricultural peatlands, and a sensitivity analysis indicated that the estimated mitigation effect achieved by raising of water table depth was robust to changes in the parameters governing evapotranspiration and organic matter decomposition. Future work is still needed to simulate N<sub>2</sub>O fluxes as accurately as CO<sub>2</sub> emissions, particularly given its high sensitivity to environmental conditions. Additionally, the model was parameterized and evaluated mainly using data representing a shallow peat layer, and future studies should be conducted to understand relationship between GHG emissions and the peat layer thickness on a more mechanistic level. The results indicate that well-drained peat soils that still retain a high carbon stock should be targeted to effectively mitigate climate change. Yet, the results also suggest that smaller reductions in annual emissions are possible in cultivated peatlands with thinned peat deposits, even with conservative changes to the water management practices.

540 *Code and data availability.* The simulations were done with the LDNDC model (v 1.36, revision 11770), which is only available from the model developers upon request. The model has been developed at KIT-Campus Alpin (<https://ldnc.imk-ifu.kit.edu/about/model.php>, last access: 22 August 2025).

The model outputs along with the flux measurements (CO<sub>2</sub>, N<sub>2</sub>O, evapotranspiration; 2019 - 2022) are archived in METIS: <https://doi.org/10.57707/FMI-B2SHARE.60ED65A7CBB04147AE3EFCE572DD8FD0>

545 The satellite data and soil moisture measurements were obtained from Field Observatory. This data can be downloaded interactively from the Field Observatory website (<https://www.fieldobservatory.org>, last access: 22 August 2025)

All other datasets used in this study are available upon request.

*Author contributions.* Conceptualization HK, SG, MN, MiL, MaL, LK, JV; Methodology DK, JV, LK, HK; Software DK, JV, HK; Formal analysis JV, HK; Investigation SG, HV, MK, MN, MiL, LK, JV, HK; Resources MaL, MiL, LK, JV, JL; Data curation SG, HV, MK, MN,



550 MiL, DK; Writing – original draft SG, MN, MiL, DK, HV, MK, LK, JV, HK; Writing – review and editing SG, MN, MiL, MaL, MK, LK, JL, JV, HK; Visualization SG, MN, MiL, HK; Supervision LK, JL, JV; Project administration LK, JV, JL; Funding acquisition LK, JL;

*Competing interests.* The authors declare no competing interests.

*Acknowledgements.* We greatly acknowledge Hermanni Aaltonen, Tuomas Laurila, and Juha Hatakka for building and maintaining the EC set-up, Olli Nevalainen for assistance with satellite observations, and the staff at Ruukki experimental station for taking care of the  
555 management practices and the support with the measurement campaigns.

This research was funded by the Strategic Research Council (SRC) established within the Research Council of Finland (grant no. 352431), the Atmosphere and Climate Competence Center funded by the Research Council of Finland (337552), Research Council of Finland (grant no. 362254), the Ministry of Agriculture and Forestry of Finland (grant no. VN/27979/2021), Business Finland (8391/31/2021), and European Research Executive Agency (REA) through the Mission Soil project MARVIC (Grant Agreement: 101112942).



## 560 References

- FMI Weather GHG Concentration, <https://en.ilmatieteenlaitos.fi/ghg-concentrations>, accessed: 2025-01-15, 2025.
- Aben, R. C. H., van de Craats, D., Boonman, J., Peeters, S. H., Vriend, B., Boonman, C. C. F., van der Velde, Y., Erkens, G., and van den Berg, M.: CO<sub>2</sub> emissions of drained coastal peatlands in the Netherlands and potential emission reduction by water infiltration systems, *Biogeosciences*, 21, 4099–4118, <https://doi.org/10.5194/bg-21-4099-2024>, 2024.
- 565 Angelo Canty and B. D. Ripley: boot: Bootstrap R (S-Plus) Functions, r package version 1.3-30, 2024.
- Barton, L., Wolf, B., Rowlings, D., Scheer, C., Kiese, R., Grace, P., Stefanova, K., and Butterbach-Bahl, K.: Sampling frequency affects estimates of annual nitrous oxide fluxes, *Scientific reports*, 5, 15 912, <https://doi.org/https://doi.org/10.1038/srep15912>, 2015.
- Berglund, Ö. and Berglund, K.: Influence of water table level and soil properties on emissions of greenhouse gases from cultivated peat soil, *Soil Biology and Biochemistry*, 43, 923–931, 2011.
- 570 Boonman, J., Hefting, M. M., van Huissteden, C. J. A., van den Berg, M., van Huissteden, J. ., Erkens, G., Melman, R., and van der Velde, Y.: Cutting peatland CO<sub>2</sub> emissions with water management practices, *Biogeosciences*, 19, 5707–5727, <https://doi.org/10.5194/bg-19-5707-2022>, 2022.
- Bridgman, S. D. and Richardson, C. J.: Mechanisms controlling soil respiration (CO<sub>2</sub> and CH<sub>4</sub>) in southern peatlands, *Soil Biology and Biochemistry*, 24, 1089–1099, [https://doi.org/10.1016/0038-0717\(92\)90058-6](https://doi.org/10.1016/0038-0717(92)90058-6), 1992.
- 575 Carstensen, M. V., Hashemi, F., Hoffmann, C. C., Zak, D., Audet, J., and Kronvang, B.: Efficiency of mitigation measures targeting nutrient losses from agricultural drainage systems: A review, *Ambio*, 49, 1820–1837, <https://doi.org/10.1007/s13280-020-01345-5>, 2020.
- Couwenberg, J., Thiele, A., Tanneberger, F., Augustin, J., Bärisch, S., Dubovik, D., Liashchynskaya, N., Michaelis, D., Minke, M., Skuratovich, A., et al.: Assessing greenhouse gas emissions from peatlands using vegetation as a proxy, *Hydrobiologia*, 674, 67–89, 2011.
- Cuddington, K., Fortin, M.-J., Gerber, L., Hastings, A., Liebhold, A., O’connor, M., and Ray, C.: Process-based models are required to  
 580 manage ecological systems in a changing world, *Ecosphere*, 4, 1–12, 2013.
- de Wit, J. A. J., Ritsema, C. J. C., van Dam, J. C. J., van den Eertwegh, G. G., and Bartholomeus, R. P. R.: Development of subsurface drainage systems: Discharge – retention – recharge, *Agricultural Water Management*, 269, 107 677, <https://doi.org/https://doi.org/10.1016/j.agwat.2022.107677>, 2022.
- Dinsmore, K. J., Skiba, U. M., Billett, M. F., and Rees, R. M.: Effect of water table on greenhouse gas emissions from peatland mesocosms,  
 585 *Plant and Soil*, 318, 229–242, 2009.
- Duarte, C., Amthor, J., De Angelis, D., et al.: The limits to models in ecology. *Models in ecosystem science*, 2003.
- Eickenscheidt, T., Heinichen, J., and Drösler, M.: The greenhouse gas balance of a drained fen peatland is mainly controlled by land-use rather than soil organic carbon content, *Biogeosciences*, 12, 5161–5184, <https://doi.org/10.5194/bg-12-5161-2015>, 2015.
- Evans, C., Peacock, M., Baird, A., Artz, R., Burden, A., Callaghan, N., Chapman, P., Cooper, H., Coyle, M., Craig, E., et al.: Overriding  
 590 water table control on managed peatland greenhouse gas emissions, *Nature*, 593, 548–552, 2021.
- Finnish Meteorological Institute: Weather station: Siikajoki-Ruukki, accessed on 30.05.2023, <https://en.ilmatieteenlaitos.fi/open-data>, 2023.
- Flessa, H., Wild, U., Klemisch, M., and Pfadenhauer, J.: Nitrous oxide and methane fluxes from organic soils under agriculture, *European Journal of Soil Science*, 49, 327–335, 1998.
- Freeman, B. W., Evans, C. D., Musarika, S., Morrison, R., Newman, T. R., Page, S. E., Wiggs, G. F., Bell, N. G., Styles, D., Wen, Y., et al.:  
 595 Responsible agriculture must adapt to the wetland character of mid-latitude peatlands, *Global Change Biology*, 28, 3795–3811, 2022.



- Gerin, S., Vekuri, H., Liimatainen, M., Tuovinen, J.-P., Kekkonen, J., Kulmala, L., Laurila, T., Linkosalmi, M., Liski, J., Joki-Tokola, E., et al.: Two contrasting years of continuous N<sub>2</sub>O and CO<sub>2</sub> fluxes on a shallow-peated drained agricultural boreal peatland, *Agricultural and Forest Meteorology*, 341, 109–630, <https://doi.org/https://doi.org/10.1016/j.agrformet.2023.109630>, 2023.
- 600 Gilhespy, S. L., Anthony, S., Cardenas, L., Chadwick, D., del Prado, A., Li, C., Misselbrook, T., Rees, R. M., Salas, W., Sanz-Cobena, A., et al.: First 20 years of DNDC (DeNitrification DeComposition): model evolution, *Ecological modelling*, 292, 51–62, 2014.
- Grote, R., Lavoie, A.-V., Rambal, S., Staudt, M., Zimmer, I., and Schnitzler, J.-P.: Modelling the drought impact on monoterpene fluxes from an evergreen Mediterranean forest canopy, *Oecologia*, 160, 213–223, 2009.
- Haas, E., Klatt, S., Fröhlich, A., Kraft, P., Werner, C., Kiese, R., Grote, R., Breuer, L., and Butterbach-Bahl, K.: LandscapeDNDC: a process model for simulation of biosphere–atmosphere–hydrosphere exchange processes at site and regional scale, *Landscape ecology*, 28, 615–636, 2013.
- 605 He, H. and Roulet, N. T.: Improved estimates of carbon dioxide emissions from drained peatlands support a reduction in emission factor, *Communications Earth & Environment*, 4, 436, 2023.
- Heikkinen, J., Lång, K., Honkanen, H., and Myllys, M.: Mitigation of Greenhouse Gas Emissions by Optimizing Groundwater Level in Boreal Cultivated Peatland, *Wetlands*, 44, 78, <https://doi.org/10.1007/s13157-024-01833-4>, 2024.
- 610 Hersbach, H., Bell, B., Berrisford, P., Hirahara, S., Horányi, A., Muñoz-Sabater, J., Nicolas, J., Peubey, C., Radu, R., Schepers, D., Simmonds, A., Soci, C., Abdalla, S., Abellan, X., Balsamo, G., Bechtold, P., Biavati, G., Bidlot, J., Bonavita, M., De Chiara, G., Dahlgren, P., Dee, D., Diamantakis, M., Dragani, R., Flemming, J., Forbes, R., Fuentes, M., Geer, A., Haimberger, L., Healy, S., Hogan, R. J., Hólm, E., Janisková, M., Keeley, S., Laloyaux, P., Lopez, P., Lupu, C., Radnoti, G., de Rosnay, P., Rozum, I., Vamborg, F., Villaume, S., and Thépaut, J.-N.: The ERA5 global reanalysis, *Quarterly Journal of the Royal Meteorological Society*, 146, 1999–2049, <https://doi.org/https://doi.org/10.1002/qj.3803>, 2020.
- 615 Huang, X., Silvennoinen, H., Kløve, B., Regina, K., Kandel, T. P., Piayda, A., Karki, S., Lærke, P. E., and Höglind, M.: Modelling CO<sub>2</sub> and CH<sub>4</sub> emissions from drained peatlands with grass cultivation by the BASGRA-BGC model, *Science of The Total Environment*, 765, 144–385, <https://doi.org/10.1016/j.scitotenv.2020.144385>, 2021a.
- Huang, Y., Ciais, P., Luo, Y., Zhu, D., Wang, Y., Qiu, C., Goll, D. S., Guenet, B., Makowski, D., De Graaf, I., et al.: Tradeoff of CO<sub>2</sub> and CH<sub>4</sub> emissions from global peatlands under water-table drawdown, *Nature Climate Change*, 11, 618–622, 2021b.
- 620 Jeewani, P. H., Brown, R. W., Rhymes, J. M., McNamara, N. P., Chadwick, D. R., Jones, D. L., and Evans, C. D.: Greenhouse gas removal in agricultural peatland via raised water levels and soil amendment, *Biochar*, 7, 1–15, <https://doi.org/https://doi.org/10.1007/s42773-024-00422-2>, 2025.
- Kandel, T. P., Gowda, P. H., and Northup, B. K.: Influence of tillage systems, and forms and rates of nitrogen fertilizers on CO<sub>2</sub> and N<sub>2</sub>O fluxes from winter wheat cultivation in Oklahoma, *Agronomy*, 10, 320, <https://doi.org/https://doi.org/10.1080/09064710.2011.614272>, 2020.
- 625 Klemetsson, L., Von Arnold, K., Weslien, P., and Gundersen, P.: Soil CN ratio as a scalar parameter to predict nitrous oxide emissions, *Global Change Biology*, 11, 1142–1147, <https://doi.org/https://doi.org/10.1111/j.1365-2486.2005.00973.x>, 2005.
- Kraus, D., Weller, S., Klatt, S., Haas, E., Wassmann, R., Kiese, R., and Butterbach-Bahl, K.: A new LandscapeDNDC biogeochemical module to predict CH<sub>4</sub> and N<sub>2</sub>O emissions from lowland rice and upland cropping systems, *Plant and Soil*, 386, 125–149, 2015.
- 630 Krause, P., Boyle, D., and Bäse, F.: Comparison of different efficiency criteria for hydrological model assessment, *Advances in geosciences*, 5, 89–97, 2005.



- Lång, K., Honkanen, H., Heikkinen, J., Saarnio, S., Larmola, T., and Kekkonen, H.: Impact of crop type on the greenhouse gas (GHG) emissions of a rewetted cultivated peatland, *Soil*, 10, 827–841, <https://doi.org/https://doi.org/10.5194/soil-10-827-2024>, 2024.
- 635 Leiber-Sauheitl, K., Fuß, R., Voigt, C., and Freibauer, A.: High CO<sub>2</sub> fluxes from grassland on histic Gleysol along soil carbon and drainage gradients, *Biogeosciences*, 11, 749–761, <https://doi.org/10.5194/bg-11-749-2014>, 2014.
- Leifeld, J. and Menichetti, L.: The underappreciated potential of peatlands in global climate change mitigation strategies, *Nature communications*, 9, 1071, 2018.
- Leifeld, J., Steffens, M., and Galego-Sala, A.: Sensitivity of peatland carbon loss to organic matter quality, *Geophysical Research Letters*, 39, <https://doi.org/10.1029/2012GL051856>, 2012.
- 640 Leppelt, T., Dechow, R., Gebbert, S., Freibauer, A., Lohila, A., Augustin, J., Drösler, M., Fiedler, S., Glatzel, S., Höper, H., et al.: Nitrous oxide emission budgets and land-use-driven hotspots for organic soils in Europe, *Biogeosciences*, 11, <https://doi.org/https://doi.org/10.5194/bg-11-6595-2014>, 2014.
- Liebermann, R., Breuer, L., Houska, T., Kraus, D., Moser, G., and Kraft, P.: Simulating long-term development of greenhouse gas emissions, plant biomass, and soil moisture of a temperate grassland ecosystem under elevated atmospheric CO<sub>2</sub>, *Agronomy*, 10, 50, 2019.
- 645 Liu, H. and Lennartz, B.: Hydraulic properties of peat soils along a bulk density gradient—A meta study, *Hydrological Processes*, 33, 101–114, 2019.
- Maljanen, M., Hytönen, J., and Martikainen, P. J.: Cold-season nitrous oxide dynamics in a drained boreal peatland differ depending on land-use practice, *Canadian journal of forest research*, 40, 565–572, <https://doi.org/https://doi.org/10.1139/X10-004>, 2010.
- 650 Mander, Ü., Espenberg, M., Melling, L., and Kull, A.: Peatland restoration pathways to mitigate greenhouse gas emissions and retain peat carbon, *Biogeochemistry*, 167, 523–543, 2024.
- Martikainen, P. J., Nykänen, H., Crill, P., and Silvola, J.: Effect of a lowered water table on nitrous oxide fluxes from northern peatlands, *Nature*, 366, 51–53, <https://doi.org/https://doi.org/10.1038/366051a0>, 1993.
- Menberu, M. W., Marttila, H., Ronkanen, A.-K., Haghighi, A. T., and Kløve, B.: Hydraulic and physical properties of managed and intact peatlands: Application of the van Genuchten-Mualem models to peat soils, *Water Resources Research*, 57, e2020WR028624, 2021.
- 655 Montanarella, L., Jones, R. J., and Hiederer, R.: The distribution of peatland in Europe., 2006.
- Mualem, Y.: A new model for predicting the hydraulic conductivity of unsaturated porous media, *Water resources research*, 12, 513–522, 1976.
- Neubauer, S. C.: Global warming potential is not an ecosystem property, *Ecosystems*, 24, 1–11, <https://doi.org/https://doi.org/10.1007/s10021-021-00631-x>, 2021.
- 660 Nevalainen, O., Niemitalo, O., Fer, I., Juntunen, A., Mattila, T., Koskela, O., Kukkamäki, J., Höckerstedt, L., Mäkelä, L., Jarva, P., et al.: Towards agricultural soil carbon monitoring, reporting, and verification through the Field Observatory Network (FiON), *Geoscientific Instrumentation, Methods and Data Systems*, 11, 93–109, <https://doi.org/https://doi.org/10.5194/gi-11-93-2022>, 2022.
- Normand, A. E., Turner, B. L., Lamit, L. J., Smith, A. N., Baiser, B., Clark, M. W., Hazlett, C., Kane, E. S., Lilleskov, E., Long, J. R., Grover, S. P., and Reddy, K. R.: Organic Matter Chemistry Drives Carbon Dioxide Production of Peatlands, *Geophysical Research Letters*, 48, e2021GL093392, <https://doi.org/10.1029/2021GL093392>, 2021.
- 665 Pärn, J., Verhoeven, J. T., Butterbach-Bahl, K., Dise, N. B., Ullah, S., Aasa, A., Egorov, S., Espenberg, M., Järveoja, J., Jauhiainen, J., et al.: Nitrogen-rich organic soils under warm well-drained conditions are global nitrous oxide emission hotspots, *Nature communications*, 9, 1–8, <https://doi.org/https://doi.org/10.1038/s41467-018-03540-1>, 2018.



- 670 Petersen, K., Kraus, D., Calanca, P., Semenov, M. A., Butterbach-Bahl, K., and Kiese, R.: Dynamic simulation of management events for assessing impacts of climate change on pre-alpine grassland productivity, *European Journal of Agronomy*, 128, 126 306, 2021.
- Pham, T., Marttila, H., Lämpikivi, M., Lötjönen, T., Aaltonen, H., Vekuri, H., Kløve, B., and Liimatainen, M.: Hydrology of a Cultivated Peatland in Northern Finland and Implications for Management, manuscript in revision.
- Premrov, A., Wilson, D., Saunders, M., Yeluripati, J., and Renou-Wilson, F.: CO<sub>2</sub> fluxes from drained and rewetted peat-
- 675 lands using a new ECOSSE model water table simulation approach, *Science of The Total Environment*, 754, 142 433, <https://doi.org/10.1016/j.scitotenv.2020.142433>, 2021.
- R Core Team: R: A Language and Environment for Statistical Computing, R Foundation for Statistical Computing, Vienna, Austria, <https://www.R-project.org/>, 2024.
- Rees, R., Augustin, J., Alberti, G., Ball, B., Boeckx, P., Cantarel, A., Castaldi, S., Chirinda, N., Chojnicki, B., Giebels, M., et al.: Nitrous
- 680 oxide emissions from European agriculture—an analysis of variability and drivers of emissions from field experiments, *Biogeosciences*, 10, <https://doi.org/https://doi.org/10.5194/bg-10-2671-2013>, 2013.
- Ridal, M., Bazile, E., Le Moigne, P., Randriamampianina, R., Schimanke, S., Andrae, U., Berggren, L., Brousseau, P., Dahlgren, P., Edvinsson, L., El-Said, A., Glinton, M., Hagelin, S., Hopsch, S., Isaksson, L., Medeiros, P., Olsson, E., Unden, P., and Wang, Z. Q.: CERRA, the Copernicus European Regional Reanalysis system, *Quarterly Journal of the Royal Meteorological Society*, 150, 3385–3411,
- 685 <https://doi.org/https://doi.org/10.1002/qj.4764>, 2024.
- Salla, A., Salo, H., Tähtikarhu, M., Marttila, H., Lämpikivi, M., Liimatainen, M., Lötjönen, T., and Koivusalo, H.: Simulating controlled drainage and hydrological connections in a cultivated peatland field, *Vadose Zone Journal*, 23, e20 387, <https://doi.org/https://doi.org/10.1002/vzj2.20387>, 2024.
- Sierra, C. A., Ceballos-Núñez, V., Hartmann, H., Herrera-Ramírez, D., and Metzler, H.: Ideas and perspectives: Allocation of carbon from
- 690 net primary production in models is inconsistent with observations of the age of respired carbon, *Biogeosciences (Online)*, 19, 3727–3738, <https://doi.org/10.5194/bg-19-3727-2022>, 2022.
- Sifounakis, O., Haas, E., Butterbach-Bahl, K., and Papadopoulou, M. P.: Regional assessment and uncertainty analysis of carbon and nitrogen balances at cropland scale using the ecosystem model LandscapeDNDC, *Biogeosciences*, 21, 1563–1581, 2024.
- Tcherkez, G., Gauthier, P., Buckley, T. N., Busch, F. A., Barbour, M. M., Bruhn, D., Heskell, M. A., Gong, X. Y., Crous, K. Y., Griffin,
- 695 K., Way, D., Turnbull, M., Adams, M. A., Atkin, O. K., Farquhar, G. D., and Cornic, G.: Leaf day respiration: low CO<sub>2</sub> flux but high significance for metabolism and carbon balance, 216, 986–1001, <https://doi.org/10.1111/nph.14816>, 2017.
- Teepe, R., Vor, A., Beese, F., and Ludwig, B.: Emissions of N<sub>2</sub>O from soils during cycles of freezing and thawing and the effects of soil water, texture and duration of freezing, *European Journal of Soil Science*, 55, 357–365, <https://doi.org/https://doi.org/10.1111/j.1365-2389.2004.00602.x>, 2004.
- 700 Tiemeyer, B., Albiac Borraz, E., Augustin, J., Bechtold, M., Beetz, S., Beyer, C., Drösler, M., Ebli, M., Eickenscheidt, T., Fiedler, S., et al.: High emissions of greenhouse gases from grasslands on peat and other organic soils, *Global change biology*, 22, 4134–4149, 2016.
- Vekuri, H., Tuovinen, J.-P., Kulmala, L., Papale, D., Kolari, P., Aurela, M., Laurila, T., Liski, J., and Lohila, A.: A widely-used eddy covariance gap-filling method creates systematic bias in carbon balance estimates, *Scientific Reports*, 13, 1720, 2023.
- Vekuri, H., Tuovinen, J.-P., Kulmala, L., Aurela, M., Thum, T., Liski, J., and Lohila, A.: Improved uncertainty estimates for eddy covariance-
- 705 based carbon dioxide balances using deep ensembles for gap-filling, *Agricultural and Forest Meteorology*, 371, 110 558, 2025.
- Vira, J., Vekuri, H., Nevalainen, O., Korkiakoski, M., Mattila, T., Aaltonen, H., Koskinen, M., Lohila, A., Pihlatie, M., and Liski, J.: Improving Agricultural Carbon Monitoring with Sentinel-2 and Eddy-Covariance-Based Plant Productivity Estimates, *Carbon Management*, 2025.



- Waddington, J. M., Morris, P. J., Kettridge, N., Granath, G., Thompson, D. K., and Moore, P. A.: Hydrological feedbacks in northern peatlands, *Ecohydrology*, 8, 113–127, <https://doi.org/10.1002/eco.1493>, 2014.
- 710 Wagner-Riddle, C., Congreves, K. A., Abalos, D., Berg, A. A., Brown, S. E., Ambadan, J. T., Gao, X., and Tenuta, M.: Globally important nitrous oxide emissions from croplands induced by freeze–thaw cycles, *Nature Geoscience*, 10, 279–283, <https://doi.org/https://doi.org/10.1038/ngeo2907>, 2017.
- Wang, C., Amon, B., Schulz, K., and Mehdi, B.: Factors that influence nitrous oxide emissions from agricultural soils as well as their representation in simulation models: A review, *Agronomy*, 11, 770, <https://doi.org/https://doi.org/10.3390/agronomy11040770>, 2021.
- 715 Wilson, D., Blain, D., Couwenberg, J., Evans, C. D., Murdiyarso, D., Page, S., Renou-Wilson, F., Rieley, J., Sirin, A., Strack, M., et al.: Greenhouse gas emission factors associated with rewetting of organic soils, 2016a.
- Wilson, D., Farrell, C. A., Fallon, D., Moser, G., Müller, C., and Renou-Wilson, F.: Multiyear greenhouse gas balances at a rewetted temperate peatland, *Global change biology*, 22, 4080–4095, 2016b.
- Yli-Halla, M., Lötjönen, T., Kekkonen, J., Virtanen, S., Marttila, H., Liimatainen, M., Saari, M., Mikkola, J., Suomela, R., and Joki-Tokola, E.: Thickness of peat influences the leaching of substances and greenhouse gas emissions from a cultivated organic soil, *Science of the Total Environment*, 806, 150 499, 2022.
- 720